Characteristics of tropospheric ozone variability over an urban site in Southeast Asia: A study based on MOZAIC and MOZART vertical profiles

L. K. Sahu,[1] Varun Sheel,[1] M. Kajino,[2] Sachin S. Gunthe,[3] Valérie Thouret,[4] P. Nedelec,[5] and Herman G. Smit[6]

Received 2 April 2013; revised 11 July 2013; accepted 17 July 2013; published 15 August 2013.

[1] The Measurement of Ozone and Water Vapor by Airbus In-Service Aircraft (MOZAIC) profiles of O_3 and CO were analyzed to study their variation in the troposphere over Bangkok. Mixing ratios of O_3 and CO were enhanced in planetary boundary layer (PBL) being highest in winter followed by summer and wet seasons. The daytime profiles of O_3 show higher values compared to nighttime observations in PBL region, but little differences were observed in the free troposphere. The decreasing mixing ratios of O_3 in the lower and upper troposphere were associated with shallow and deep convections, respectively. Back trajectory and fire count data indicate that the seasonal variations in trace gases were caused mainly by the regional shift in long-range transport and biomass-burning patterns. In wet season, flow of oceanic air and negligible presence of local biomass burning resulted in lowest O_3 and CO, while their high levels in dry season were due to extensive biomass burning and transport of continental air masses. The Model for Ozone and Related Chemical Tracers (MOZART) underestimated both O_3 and CO in the PBL region but overestimated these in the free troposphere. Simulations of O_3 and CO also show the daytime/nighttime differences but do not capture several key features observed in the vertical distributions. The observed and simulated values of O_3 and CO during September–November 2006 were significantly higher than the same period of 2005. The year-to-year differences were mainly due to El Niño-led extensive fires in Indonesia during 2006 but normal condition during 2005.

Citation: Sahu, L. K., V. Sheel, M. Kajino, S. S. Gunthe, V. Thouret, P. Nedelec, and H. G. Smit (2013), Characteristics of tropospheric ozone variability over an urban site in Southeast Asia: A study based on MOZAIC and MOZART vertical profiles, *J. Geophys. Res. Atmos.*, *118*, 8729–8747, doi:10.1002/jgrd.50662.

1. Introduction

[2] Troposphere ozone (O_3) plays a key role in the Earth's climate and environment. In the troposphere, O_3 is a greenhouse gas because of strong absorption of infrared (IR) radiation centered at 9.6 μm and hence contributes to the global warming [*Forster and Shine*, 1997; *Gauss et al.*, 2003]. Tropospheric O_3 is the third most important contributor to the positive radiative forcing with estimates of about +0.35 W m^{-2} [*Intergovernmental Panel on Climate Change*, 2007]. The increasing emissions of various precursor gases can enhance the global concentration of O_3 in the troposphere. Anthropogenic activities like biomass burning and combustion of biofuel and fossil fuel are the major sources of carbon monoxide (CO), methane (CH_4), oxides of nitrogen ($NO_x = NO + NO_2$), and volatile organic compounds (VOCs) in Asia [*Cooper et al.*, 2010; *Lamarque et al.*, 2010; *Sahu*, 2012]. For example, the recent bottom-up inventories indicate that South and East Asia's NO_x emissions increased about 44% during 2001–2006. The regional inventories of various O_3 precursors in Asia emitted from the anthropogenic sources are reported in several studies [*Olivier et al.*, 2002; *Heald et al.*, 2003]. Emissions of many O_3 precursors are increasing rapidly due to the fast industrialization, urbanization, and population growth [*Streets et al.*, 2003a; *Ohara et al.*, 2007]. The impact of these emissions, especially from the developing countries in the tropics, on the global chemistry and climate has been clearly attributed in several research studies.

[1]Physical Research Laboratory, Ahmedabad, India.
[2]Meteorological Research Institute, Japan Meteorological Agency, Tsukuba, Japan.
[3]Environmental and Water Resources Engineering Division, Department of Civil Engineering, Indian Institute of Technology Madras, Chennai, India.
[4]Laboratoire d'A'erologie, CNRS, Observatoire Midi-Pyr'en'ees, UMR 5560, Toulouse, France.
[5]Laboratoire d'Aérologie, Unité Mixte de Recherche 5560, Centre National de la Recherche Scientifique/Université Paul Sabatier, Observatoire Midi-Pyrénées, Toulouse, France.
[6]Institute for Chemistry of the Polluted Atmosphere, Research Center Jülich, Jülich, Germany.

Corresponding author: L. K. Sahu, Space and Atmospheric Sciences Division, Physical Research Laboratory, Navrangpura, Ahmedabad 380009, India. (lokesh@prl.res.in, l_okesh@yahoo.com)

2169-897X/13/10.1002/jgrd.50662

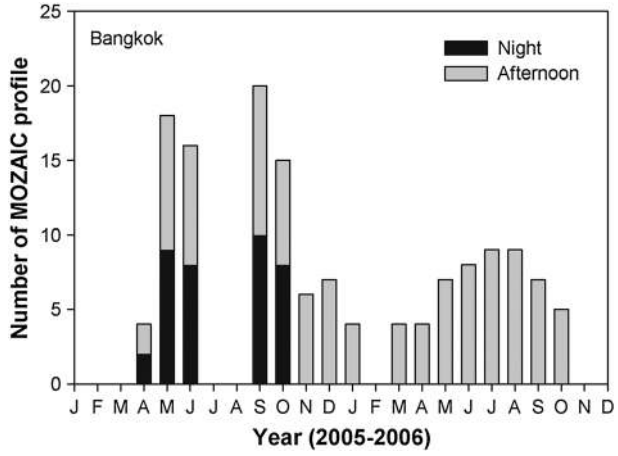

Figure 1. Monthly histogram of the number of MOZAIC profiles measured over Bangkok during the years 2005 and 2006.

[3] Typically, the emissions from vehicular traffic and industrial sources are year-round and do not show significant seasonality. On the other hand, the location and timing of emission from biomass-burning sources are different than those from anthropogenic activities. The emissions from biomass-burning sources in South and Southeast Asia (S-SE Asia) exhibit strong seasonality with a primary peak during February–April and secondary peak in August–October [*van der Werf et al*., 2006, 2010]. The long-range transport of O_3 and its various precursors from the different regions in Asia has been observed to impact the remote regions of the troposphere [*Lelieveld et al*., 2001; *Cooper et al*., 2004; *Sahu et al*., 2006; *Lal et al*., 2007]. The global model simulations and observations have attributed the increasing O_3 trend in the free troposphere over western U.S. to the rising emissions in Asia [*Cooper et al*., 2010; *Zhang et al*., 2008]. For example, the Asian pollution contributes about 3–10 ppbv to the background O_3 in the western U.S. during the spring season [*Vingarzan*, 2004; *Lin et al*., 2012]. In Asia, the measurements of O_3 are limited to study the surface variation of O_3 at several locations [*Chandra et al*., 2003; *Kumar et al*., 2012]. On the other hand, the vertical measurements of tropospheric O_3 are reported for a few locations [*Logan*, 1999; *Fujiwara et al*., 2000; *Chan et al*., 2003; *Oltmans et al*., 2006]. In recent years, measurements over several tropical stations in Asia have been reported under the Southern Hemisphere Additional Ozonesondes (SHADOZ) program [*Thompson et al*., 2003]. The vertical distributions of O_3 show large variability in the global troposphere. The major factors that determine the vertical structure of O_3 are in situ production/loss, deep convective outflow, vertical advection, shallow convection, stratosphere-troposphere exchange (STE), convective downdraft, convective overshooting, and Kelvin waves [*Sherwood and Dessler*, 2003; *Folkins et al*., 2002]. In tropical regions, the atmospheric convection is an important force for the transport of air mass from surface to the upper troposphere. In the tropics, the photochemical reactions are dominated by the cycles of O_3 and water vapor (H_2O). Ozone is photodissociated by the shortwave solar radiation (<340 nm) into electronically excited O(^1D) atoms which react with H_2O to form hydroxyl (OH) radical. The photochemical production in the tropical region is a large contributor to the global budget of O_3 in the troposphere. The lifetime of O_3 varies from 2–5 days in the tropical marine boundary layer (MBL) to approximately 90 days in the free troposphere [*Fishman et al*., 1991; *Lawrence et al*., 2003].

[4] The impact of biomass burning in S-SE Asia on tropospheric loading of O_3 over different regions of the globe has been studied mainly using the satellite and model data [*Thompson et al*., 2001; *Zhang et al*., 2011]. In S-SE Asia region, the vertical distribution of O_3 over Indonesia, Malaysia, and Hong Kong has shown the impact of biomass burning [*Chan et al*., 2003; *Yonemura et al*., 2002; *Thompson et al*., 2003]. For example, the pronounced enhancements in the total tropospheric O_3 from 20 to 55 Dobson unit (DU) were observed at Watukosek during extensive forest fires in Indonesia during year 1997 [*Fujiwara et al*., 1999]. The Measurement of Ozone and Water Vapor by Airbus In-Service Aircraft (MOZAIC) profiles of O_3 over metro cities of Delhi and Chennai in India show the impact of biomass burning [*Sahu et al*., 2009a; *Sahu et al*., 2010].

[5] The present paper is based on the vertical profiles of O_3 and CO over Bangkok using the MOZAIC measurements during years 2005 and 2006. The primary objective of this study is to understand the roles of different atmospheric processes in the distribution of O_3. Carbon monoxide has been used to investigate the impact of emissions and long-range transport due to its longer atmospheric lifetime and direct release from biomass-burning sources. *Sahu et al*. [2013] have already presented the general features of CO distributions over Bangkok. We have also used the meteorological parameters, fire count, and back trajectory data. A comparison between the MOZAIC observations and the Model for Ozone and Related Chemical Tracers-4 (MOZART-4) simulations of O_3 and CO has also been presented.

2. Description of MOZAIC Program and MOZART Model

[6] The MOZAIC project was initiated by the European scientists, aircraft manufacturers, and airliners in the year 1993 to study the variability of the chemical composition of the atmosphere [*Marenco et al*., 1998]. The MOZAIC flights have been sponsored by the Air France, Austrian Airlines, Lufthansa, and Sabena/Air France. Measurements on board Airbus A340s in scheduled flights have been operational since August 1994. In the second phase (1997–2000), measurements of O_3 and H_2O were continued while sensors for CO and of total odd-nitrogen (NO_y) were developed for the onboard deployment. The O_3 analyzer is a dual beam ultraviolet (UV) absorption instrument from Thermo-Electron (Model 49-103), which has a detection limit of 2 ppbv. Overall, the upper limit of error in the measurements of O_3 was estimated to be $\pm$(2 pbbv + 2%) [*Thouret et al*., 1998a, 1998b]. The response time of O_3 analyzer is 4 s which translates into a vertical resolution of 30 m altitude. The detailed description of sampling procedure, measurement technique, calibration, instrument validation, and quality testing is reported in *Thouret et al*. [1998b]. The measurements taken during both takeoff and landing of the aircraft have been used as vertical profile data. In this study, we have used a total of 143 profiles measured during the years 2005 and 2006. The monthly histogram of number of profiles is shown in

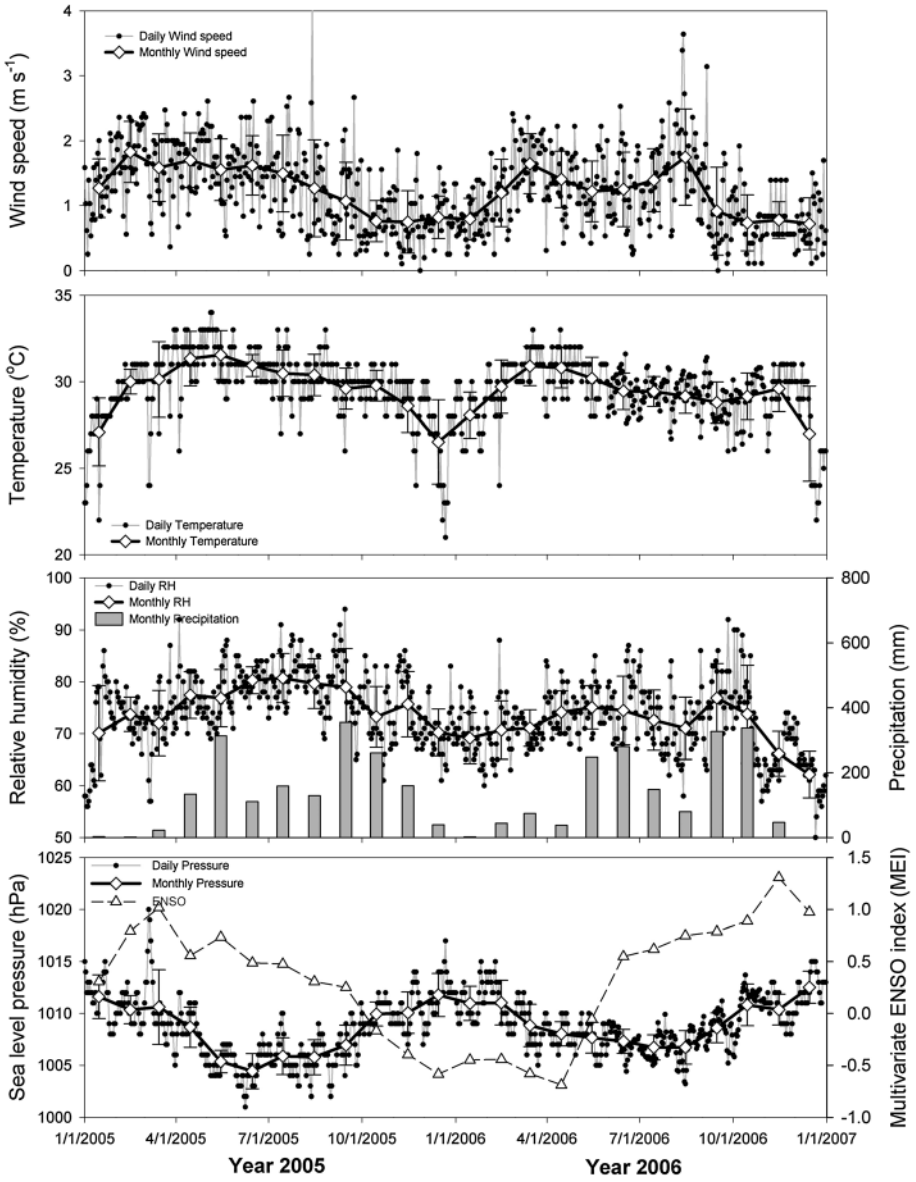

Figure 2. Time series variations of daily and monthly meteorological data at Bangkok during the years 2005 and 2006.

Figure 1. The MOZAIC profiles were measured during both daytime (13–14 h, local time (LT)) and nighttime (21–22 h, LT) on each available date of year 2005, while the measurements during year 2006 were made only during the daytime (14–15 h, LT). Therefore, to be consistent with the timing, we have used daytime profiles for the comparison between 2005 and 2006 observations. The difference between daytime and nighttime profiles for year 2005 has been discussed briefly.

[7] The MOZART is a three-dimensional (3-D) global chemical transport model of atmospheric composition to simulate the chemical and transport processes in the troposphere. The MOZART-4 version used in this study includes detailed chemistry, improved scheme for the determination of albedo, aerosols, and online calculations of photolysis rates, dry deposition, H_2O concentration, and biogenic emissions [*Horowitz et al*., 2003]. A comprehensive tropospheric chemistry with 85 gas-phase species, 12 bulk aerosol species, 39 photolysis, and 157 gas-phase reactions has been included [*Emmons et al*., 2010]. We have used the Global Forecast System (GFS) meteorological fields from the National Centers for Environmental Prediction (NCEP). The inventories for major anthropogenic sources are taken from the Precursors of Ozone and Their Effect on the Troposphere (POET) data [*Granier et al*., 2004]. The POET is based on the European projects of the Global Emission Inventory Activity (GEIA) and the Emissions Database for Global Atmospheric Research (EDGAR) [*Olivier et al*., 2003, 2005]. The POET data gridded at $1° \times 1°$ include the emissions from anthropogenic activities, biomass burning (fire), and natural sources. The representation of emissions for fire and natural sources is monthly, while anthropogenic emissions are on annual basis. Anthropogenic emissions for Asia have been updated using the Regional Emission inventory in Asia (REAS) data developed by *Ohara et al*. [2007]. The monthly average biomass-burning emissions are taken

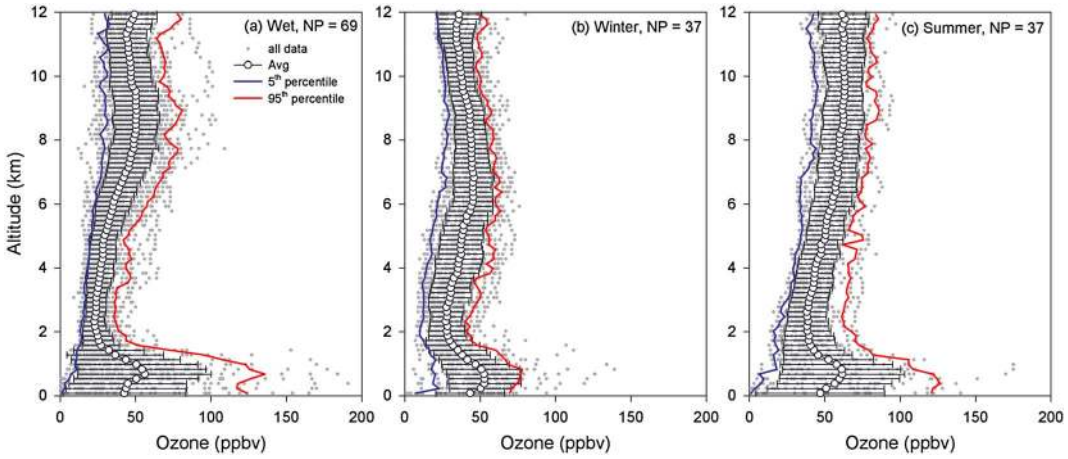

Figure 3. The MOZAIC profiles of O_3 using 150 m height interval data and their average, 5th percentile, and 95th percentile over Bangkok during the different seasons of the years 2005 and 2006. NP represents number of MOZAIC profiles.

from the Global Fire Emission Database, version 2 (GFED-v2) [*van der Werf et al*., 2006, 2010]. The model outputs are at a resolution of 2.8° × 2.8° with 28 sigma pressure levels from the surface to about 2 mbar level. We run the MOZART model on the 3 Terraflop HPC Linux cluster with 20 nodes in our institute (Physical Research Laboratory) [*Sheel et al*., 2010]. The purpose is to test performance of the model in S-SE Asia by comparing with MOZAIC data. However, these comparisons do not form the basis to study the variability in O_3 and CO over Bangkok.

3. Site and Local Emission Sources in Bangkok

[8] Bangkok is the capital city of Thailand with an area of about 1569 km^2 situated on the eastern bank of Chao Phraya River near the Gulf of Thailand. It is one of the leading economic cities in SE Asia region. Bangkok and five surrounding provinces namely Samut Prakarn, Nonthaburi, Pathumthani, Nakorn Pathom, and Samut Sakorn are known as the Bangkok Metropolitan Region (BMR). The BMR has a total population of about 14 million (as of consensus in 2010) which comprises about 22% of the Thailand's population. The international airport (Suvarnbhumi, 13.72°N, 100.48°E) is located at a distance of about 33 km in the southeast (SE) direction from the Bangkok city center. The distance from the Suvarnbhumi airport to the Gulf of Thailand is about 22 km. There are over 5.4 million vehicles running on the roads of Bangkok [*Department of Land Transport* (*DLT*), 2008]. Emissions from the vehicular traffic make dominant contribution to the air pollution in the city. Other sources like emissions from the Don Muang airport and small industrial estates also contribute to the levels of various pollutants in Bangkok. The vehicular traffic in Bangkok consists of motorcycle (40%), three-wheeler or "tuktuk" (0.2%), car (37%), taxi (1.6%), van/pickup (18%), bus (0.6%), and truck (1.8%) [*DLT*, 2010]. Although the vehicular traffic in the city has been increasing with an average of about 7% yr^{-1} since year 1989, the levels of various pollutants in Bangkok have been monitored to show a steady decline from 1992 to 2005 [*Bangkok Metropolitan Administration*, 2009]. The activities of open biomass and agricultural waste burning in the surrounding regions of Bangkok also add to the levels of various pollutants but mainly in the dry season [*Chuersuwan et al*., 2008]. About 90% of rice straw is burned from November to April, but this activity is particularly extensive during the months of February and March [*Tipayarom and Kim Oanh*, 2007]. Among the countries in SE Asia region, the number of registered vehicles is highest in Thailand but the amount of fuel and biomass burned was estimated to be second highest after Indonesia [*Streets et al*., 2003a, 2003b].

4. General Circulation and Meteorology

[9] There are three main seasons in Thailand, namely, wet (June to September), winter (October to February), and summer (March to May) [*Pochanart et al*., 2003; *Sahu et al*., 2011]. The period from winter to summer is also known as the dry season. The large-scale circulation in S-SE Asia is primarily driven by the seasonal progression of the Intertropical Convergence Zone (ITCZ) [*Asnani*, 2005]. The wet and winter seasons are associated with the northward and southward progressions of the ITCZ, respectively. The southwest (SW) wind flow brings cleaner marine air from the Indian Ocean in the wet season. On the other hand, the winds from the northeast (NE) and northwest (NW) directions transport continental

Table 1. The Seasonal Means and Ranges of 5th–95th Percentile of Tropospheric O_3 Over Bangkok During the Years 2005 and 2006

	Wet		Winter		Summer	
Altitude (km)	Mean (ppbv)	5th–95th Percentile (ppbv)	Mean (ppbv)	5th–95th Percentile (ppbv)	Mean (ppbv)	5th–95th Percentile (ppbv)
0–2	41 ± 29	9–100	43 ± 22	17–76	50 ± 33	13–101
2–4	25 ± 7	16–39	30 ± 12	12–52	40 ± 13	24–64
4–6	31 ± 10	20–48	39 ± 14	19–62	50 ± 12	33–70
6–8	43 ± 14	27–69	45 ± 12	25–64	58 ± 13	38–77
8–10	50 ± 14	29–73	41 ± 10	28–57	62 ± 12	43–81
10–12	46 ± 13	30–70	36 ± 10	23–53	62 ± 13	41–81

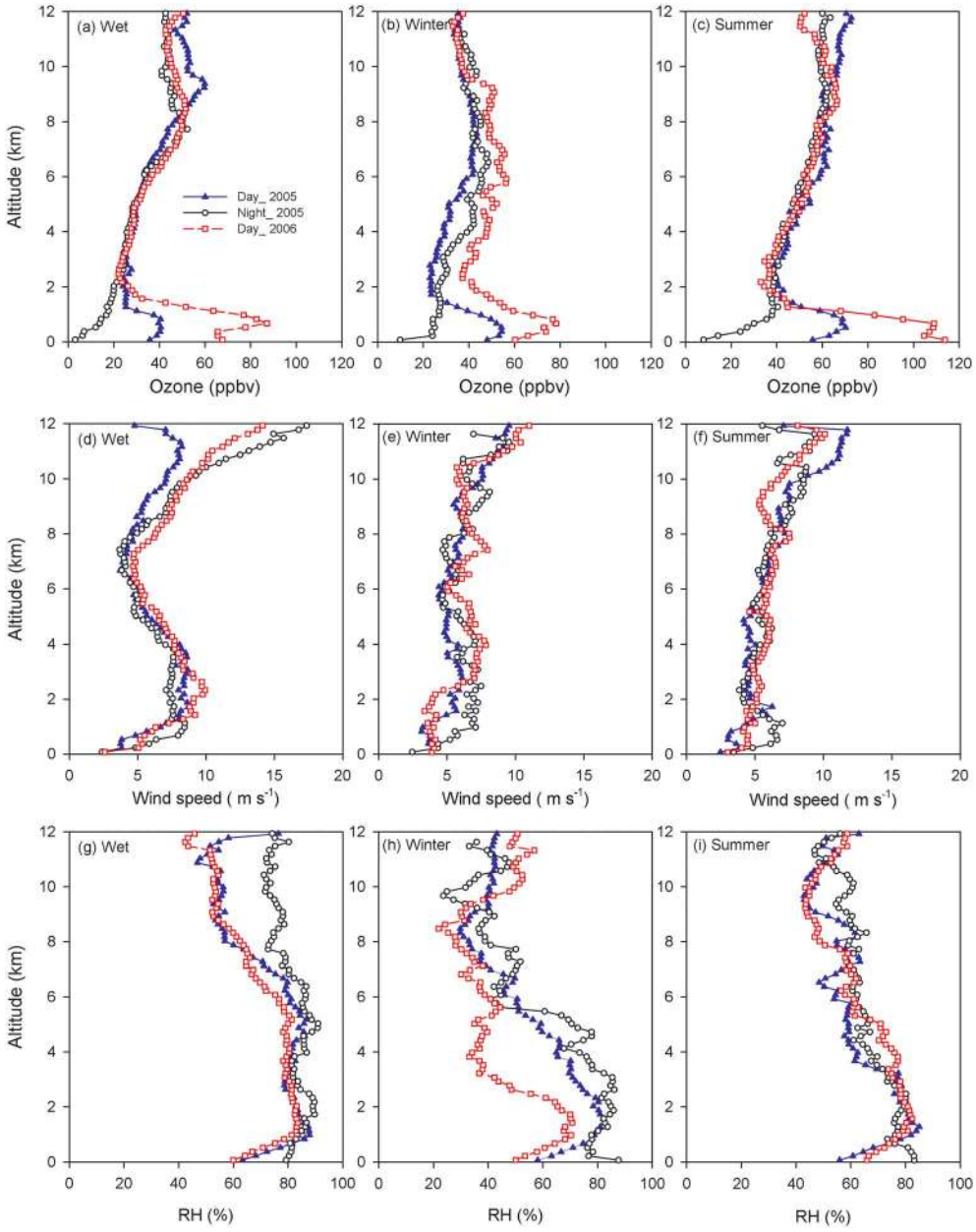

Figure 4. The mean MOZAIC profiles of (a–c) O_3, (d–f) wind speed, and (g–i) relative humidity (RH) separately for the daytime and nighttime observations over Bangkok during different seasons of the years 2005 and 2006.

pollutants in the winter season. In addition to the seasonal movement of the ITCZ, the large-scale climatic phenomena like El Niño and La Niña have been known to impact several aspects of life and environment in the SE Asia. The El Niño–Southern Oscillation (ENSO) is the Earth's strongest climate fluctuation and has global impacts [*Allan et al*., 1996]. Many countries in this region have been affected adversely by the El Niño but reported to be the most severe in Indonesia.

[10] The time series of the surface level wind speed, relative humidity (RH), pressure, temperature, and total rainfall from January 2005 to December 2006 are shown in Figure 2. The meteorological data recorded at the Don Muang Airport (DMK) in Bangkok are taken for the present study (source: http://www.wunderground.com). Almost all meteorological parameters show significant day-to-day variability in Bangkok. The monthly mean temperature varied from a minimum of 27°C in the month of December to a maximum of 32°C in March. The monthly

Table 2. The Seasonal Stability Conditions Derived Using the Equivalent Potential Temperatures in the Different Regions of the Troposphere Over Bangkok

Stability Condition	Layers (km) in the Troposphere		
	Wet Season	Winter Season	Summer Season
$(\partial\theta_e/\partial z) < 0$	0–2.8	0–2.4	0–3.5
$(\partial\theta_e/\partial z) \approx 0$	2.8–4.2	2.4–3.7	3.5–4.4
$(\partial\theta_e/\partial z) > 0$	4.2–12	3.7–12	4.4–12

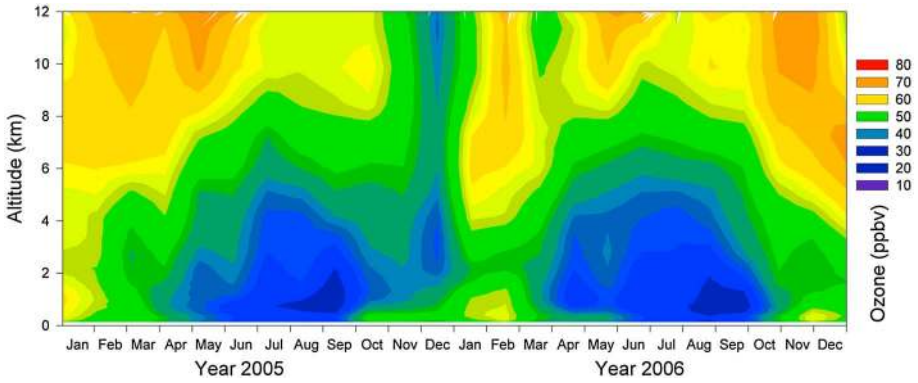

Figure 5. Contour plots of monthly mean MOZART-4 simulations of tropospheric O_3 over Bangkok for the years 2005 and 2006, respectively.

wind speed varied in the range of 1.0–2.0 m s^{-1} in the wet season; however, rather calm condition (<1.0 m s^{-1}) prevailed during the winter months. The sea level pressure varied in the ranges of 1004–1012 and 1006–1012 hPa during the years 2005 and 2006, respectively. The total annual rainfalls at Bangkok were 1685 and 1623 mm during the years 2005 and 2006, respectively. Bangkok city is very humid (>60%) throughout the year with lowest and highest levels of RH observed during winter and wet seasons, respectively. The monthly RH varied in the ranges of 70–81% and 62–79% during the years 2005 and 2006, respectively. It is important to mention that the levels of RH during the October–December period of 2006 were about 10%–15% lower during the same period of year 2005. Based on the analysis of meteorological data reordered at Bangkok during January 2002 to December 2004, the daily average depths of the planetary boundary layer (PBL) were 860, 990, and 940 m for the wet, winter, and summer seasons, respectively [*Sahu et al*., 2011 and references therein]. The ENSO is parameterized as the multivariate ENSO Index (MEI). The MEI is computed based on six different variables: sea level pressure, wind components, sea surface temperatures (SST), air temperatures, and total cloudiness fraction of the sky. As shown in Figure 2, the time series variation of Multivariate ENSO Index (MEI) indicates that the year 2005 was normal but 2006 was an El Niño year. The large positive values of MEI from August to December of year 2006 compared to the same period of year 2005 highlight the effect of the prevailing ENSO during year 2006. The ENSO-induced biomass burning, which occurs on the islands of Indonesia and Malaysia, makes SE Asia region unique in terms of the extreme interannual variability.

5. Results

5.1. Vertical Profiles of O_3

[11] The MOZAIC vertical profiles of O_3 over Bangkok for the three different seasons of the years 2005 and 2006 are shown in Figure 3. All the data points with 150 m height interval, their averages, and 5th and 95th percentiles are plotted for each season. In the PBL region, the average mixing ratios of O_3 were 41 ± 29, 43 ± 22, and 50 ± 33 ppbv in the wet, winter, and summer seasons, respectively. However, there are several data points which exceeded 100 ppbv levels in all the seasons. The annual averages of hours of O_3 exceeding 100 ppbv in Bangkok were 37–169 h yr^{-1} from 1996 to 2000 with highest for an El Niño year [*Zhang and Kim Oanh*, 2002]. The mixing ratio of O_3 increased slightly up to about 1 km and then decreased rapidly up to about 2 km altitudes. The mixing ratios of O_3 were lowest between 2 and 4 km altitudes with the averages of 25 ± 7, 30 ± 12, and 40 ± 3 ppbv for the wet, winter, and summer seasons, respectively. At higher altitudes (>4 km), the mixing ratio of O_3 showed different levels of enhancement depending on the season. In the wet season, the enhancements were mostly between 7 and 9 km altitudes. In the

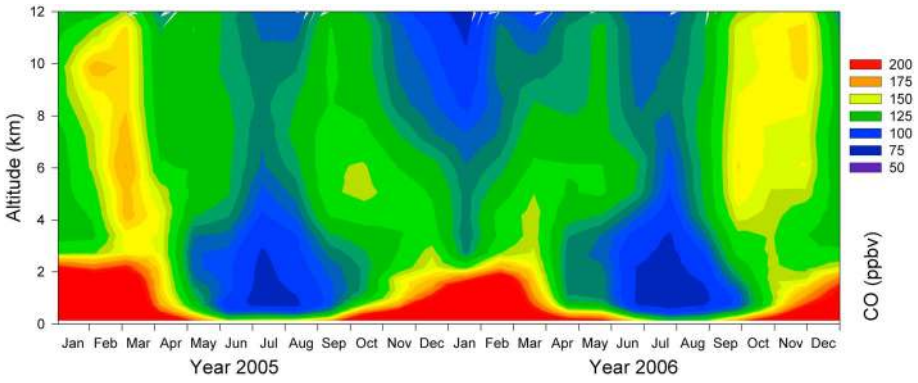

Figure 6. Contour plots of monthly mean MOZART-4 simulations of tropospheric CO over Bangkok for the years 2005 and 2006, respectively.

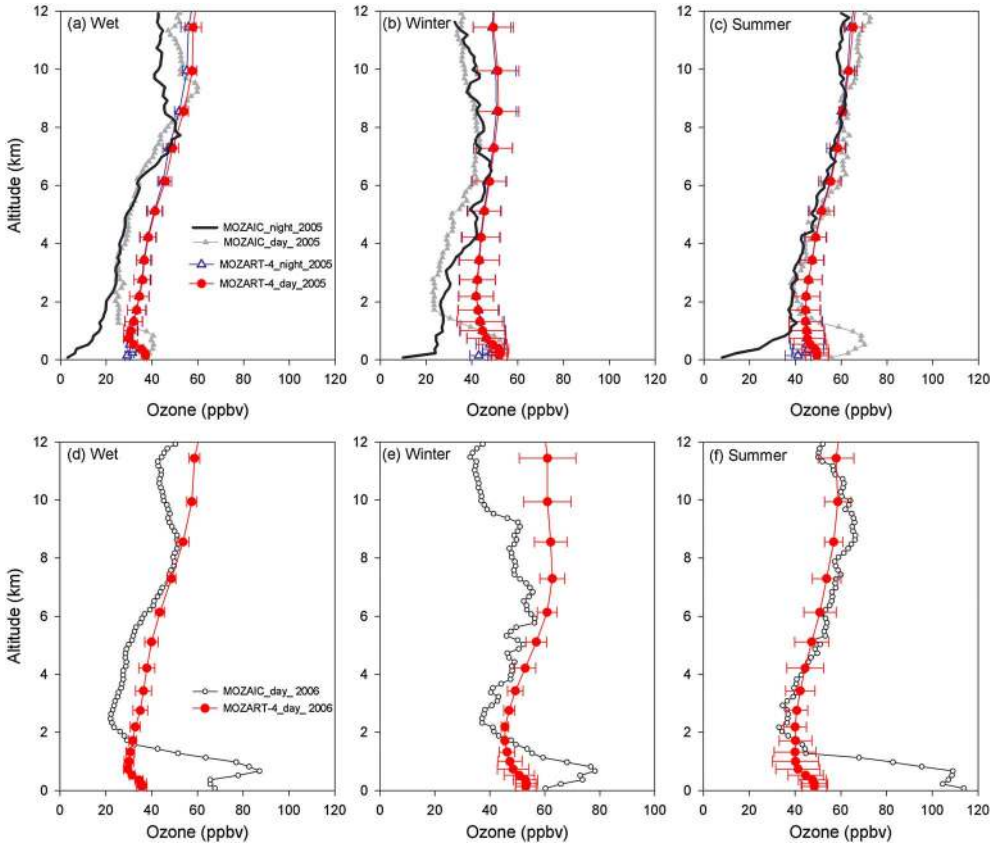

Figure 7. Comparisons between the daytime and nighttime MOZAIC and MOZART-4 profiles of O_3 over Bangkok during different seasons of the years (a–c) 2005 and (d–f) 2006.

winter season, the enhancements were observed between 4 and 8 km altitudes. In the upper troposphere, the mixing ratio of O_3 tends to decrease between 9 and 12 km altitudes. In the summer season, the profiles of O_3 showed monotonically increasing trend between 4 and 12 km altitudes. The seasonal mean mixing ratios of O_3 for the different vertical regions of the troposphere over Bangkok are presented in Table 1.

[12] The separation between two bounding profiles of 5th and 95th percentiles varies with the altitude indicating the different ranges of variation in the tropospheric O_3 over Bangkok. The 5th–95th percentile data of O_3 for the different regions of the troposphere are presented in Table 1. In the lower troposphere, the large variations in O_3 were observed throughout the year. In the PBL region, the variability in O_3 during the wet (9–100 ppbv) and summer (13–101 ppbv) seasons was more pronounced than that observed in the winter (17–76 ppbv). The highest 95th percentile in wet season was due to extensive biomass burning in Indonesia and Malaysia mainly during the year 2006. The profile of the 5th percentile has been assumed as the background profile of O_3 in the troposphere for a given season [*Sahu et al*., 2009b; *Sahu et al*., 2011]. The background mixing ratio of O_3 increased with the altitude and was 9–30, 12–28, and 13–43 ppbv in the wet, winter, and summer seasons, respectively.

[13] The seasonal mean profiles of O_3, wind speed, and RH observed over Bangkok for years 2005 (both daytime and nighttime) and 2006 (daytime only) are shown separately in Figure 4. The nighttime mixing ratios of O_3 remained below 20, 30, and 40 ppbv levels during the wet, winter, and summer seasons, respectively. However, depending on the season, the daytime profiles of O_3 showed higher values of 40–80 ppbv in the PBL region. The difference between the nighttime and daytime profiles of O_3 was highest during the summer season. Similarly, the differences between the nighttime and daytime profiles of several meteorological parameters can also be noticed (Figures 4d–4i). For example, the daytime enhancements of O_3 in the PBL region were associated with the lower values of RH and wind speed and just opposite during the nighttime. A similar comparison for the year 2006 has not been presented as the MOZAIC profiles were measured during the daytime only. We have investigated the roles of the convective transport in the distributions of O_3 using the derived parameters like equivalent potential temperature (EPT, θ_e) and lapse rate (LR) (Table 2).

[14] The results obtained from the separate analyses of MOZAIC data for the years 2005 and 2006 provide an opportunity to investigate the difference in O_3 during normal and ENSO years of observations over Bangkok. The daytime seasonal mean profiles of O_3 for the years 2005 and 2006 exhibit several key differences. Although the shape of O_3 profiles during both years remained almost the same, the mixing ratios of O_3 during year 2006 were higher compared to year 2005. The major differences due to ENSO were noticed in the lower troposphere during all the seasons. In comparison to the year 2005, the daytime surface mixing ratios of O_3 during year 2006 were higher by about 25, 15, and 40 ppbv during the wet, winter, and summer seasons, respectively. Similarly, the differences in the daytime profiles of RH for

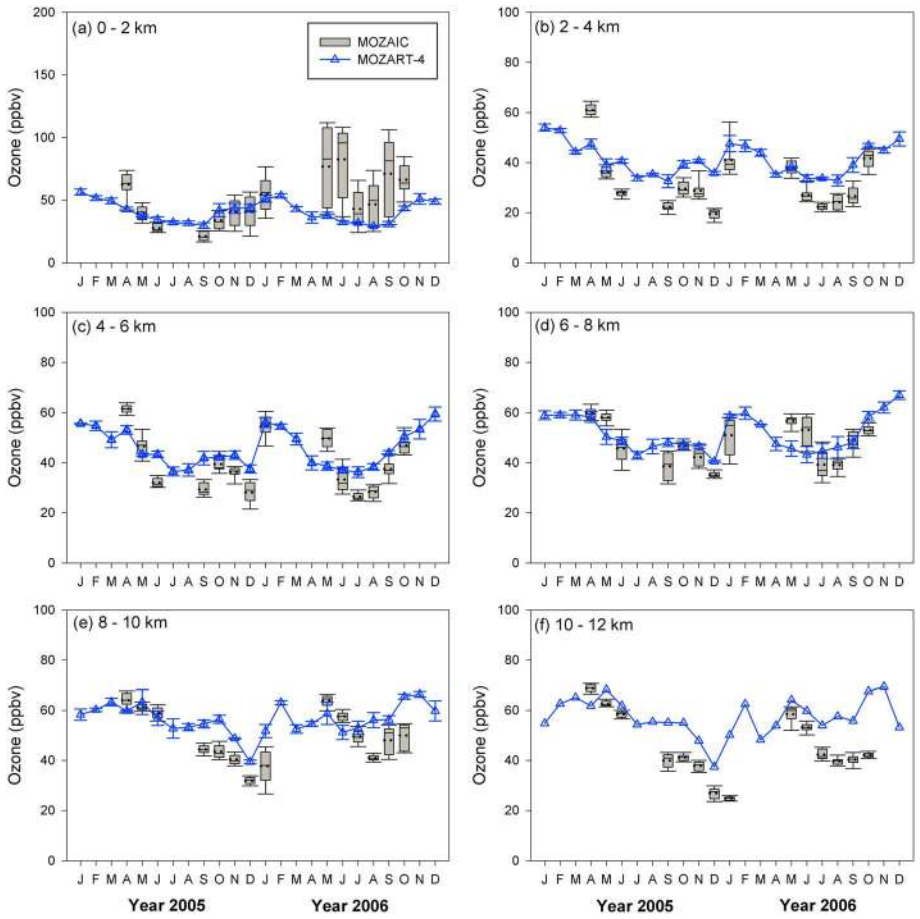

Figure 8. The monthly mixing ratios of O_3 using MOZAIC data in the different regions of the troposphere. The MOZART-4 simulations are also plotted for the comparison.

the winter season can also be noticed between normal and ENSO years of observations. In the lower and middle troposphere, the profiles of RH show higher and lower values of 50–80% and 30–70% during the winter season of years 2005 and 2006, respectively. We have investigated if these year-to-year variations observed in O_3 and meteorological parameters were caused by the normal condition and El Niño during the years 2005 and 2006, respectively. The largest increases in O_3 are not directly in the source regions but rather in the outflow of southern Asia. This is because of the time needed for photochemical production of O_3 from its precursors [*Lawrence et al*., 2003].

5.2. MOZART-4 Simulations of O_3 and CO

[15] The monthly mean MOZART-4 contour plots of tropospheric O_3 over Bangkok for the years 2005 and 2006 are shown in Figure 5. In the lower troposphere, the mixing ratio of O_3 varies in the range of 20–60 ppbv with the low and high values simulated for the wet and winter seasons, respectively, during the year 2005. In the year 2006, except for the relatively low values in summer, the seasonal pattern of O_3 in the lower troposphere was almost the same as that for the previous year. However, the simulations of O_3 in the middle and upper troposphere show distinct seasonal patterns for the years 2005 and 2006. In the year 2005, the mixing ratios were in the range of 60–70 ppbv between 6 and 12 km altitudes during the late winter and summer seasons. In this region of the troposphere, the levels of O_3 were moderate at 50–60 ppbv in the wet season and lower at 30–40 ppbv in the early winter months. However, in contrast to the year 2005, the simulations in the middle and upper troposphere show higher O_3 values (>70 ppbv) during the late wet and early winter months of year 2006. The mixing ratios of O_3 at 9–12 km altitudes during early winter months of year 2006 were higher by about 20 ppbv than those in the same period of year 2005. The elevated levels of tropical tropospheric O_3 observed by the Tropospheric Emission Spectrometer (TES) over SE Asia region during year 2006 support the impact of extensive biomass burning in the upper tropospheric O_3 over Bangkok [*Nassar et al*., 2009]. The Microwave Limb Sounder (MLS) observations also showed enhanced levels of O_3 in the tropical upper troposphere over SE Asia region due to extensive Indonesian fires in the year 2006 [*Zhang et al*., 2011].

[16] The MOZART-4 simulations of CO over Bangkok were also performed for the years 2005 and 2006. The monthly mean MOZART-4 contour plots of tropospheric CO for both the years are shown in Figure 6. In the lower troposphere, the mixing ratios of CO were in the ranges of 150–400 ppbv during the winter and summer seasons and lower values of 80–110 ppbv during the wet season. The simulations of CO in the middle and upper troposphere show

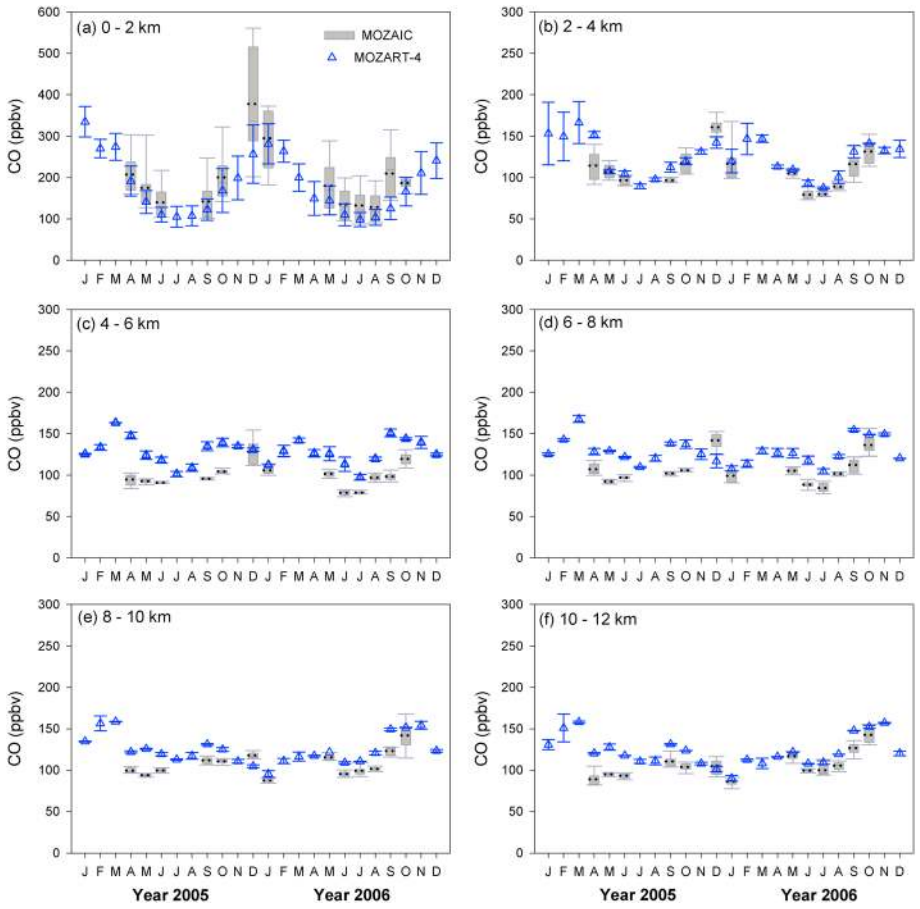

Figure 9. The monthly mixing ratios of CO using MOZAIC data in the different regions of the troposphere. The MOZART-4 simulations are also plotted for the comparison.

distinct seasonal patterns for the years 2005 and 2006. In the year 2005, the mixing ratios of CO were in the range of 150–180 ppbv between 6 and 12 km altitudes during the late winter and early summer months. In this region of the troposphere, lower values of 100–140 ppbv were simulated for the summer months. In the year 2006, the seasonal pattern of CO in the lower troposphere was similar to that of the year 2005. However, in contrast to the year 2005, the simulations of CO for year 2006 in the middle and upper troposphere show lower values (<125 ppbv) and higher values (>160 ppbv) during the summer and early winter seasons, respectively. The mixing ratios of CO at 9–12 km altitudes during early winter months of year 2006 were higher by about 50 ppbv than those for the same period of year 2005. Similar seasonal patterns of O_3 and CO with the enhancements during October and November months of year 2006 over Bangkok clearly indicate the impact of extensive biomass burning in Indonesia caused by the El Niño. In the tropical upper troposphere, fire-related emissions are transported northeastward to SE Asia by the western North Pacific subtropical high. The MLS data averaged over 100°E–125°E of longitudes show widespread enhancements of CO at 215 hPa (~11 km) between 20°S and 20°N of latitudes during year 2006 [*Zhang et al*., 2011; *Nara et al*., 2011]. The enhancements in the mixing ratio of CO were also observed over SE Asia during Indonesian forest fires in the year 2006 by the Atmospheric Chemistry Fourier Transform Spectrometer (ACEFTS), Atmospheric Infrared Sounder (AIRS), and MOPITT instruments [*Yurganov et al*., 2008; *Nara et al*., 2011; *Srivastava and Sheel*, 2012]. The substantial increase in CO mixing ratios was detected over the western tropical Pacific Ocean by the shipboard observations during ENSO 2006. In contrast to the present study, the enhancement of O_3 relative to CO was lower over Pacific Ocean suggesting that net O_3 production was not efficient in the burning plumes transported in the lower troposphere [*Nara et al*., 2011]. In addition to the combustion properties (smoldering/flaming) of biomass-burning sources in Indonesia, the difference could also be due to the different behaviors of local photochemistry in PBL and MBL.

[17] We have estimated the differences in the nighttime and daytime MOZART-4 profiles of both O_3 and CO for the year 2005. In agreement with the observations, the major differences in the mixing ratios of both the trace gases can be noticed in the lower troposphere. The enhanced mixing ratio of CO during the nighttime suggests accumulation due to the shallow PBL over Bangkok. On the other hand, the enhanced mixing ratio of O_3 during the daytime indicates the contribution of photochemical production in the presence of sunlight. The disagreement between MOZAIC and model results in the diurnal variation of O_3 in PBL could be due to the underestimation of levels of NO and O_3 titrations in MOZART-4 at Bangkok. This will lead to nonzero mixing ratios of O_3 at nighttime.

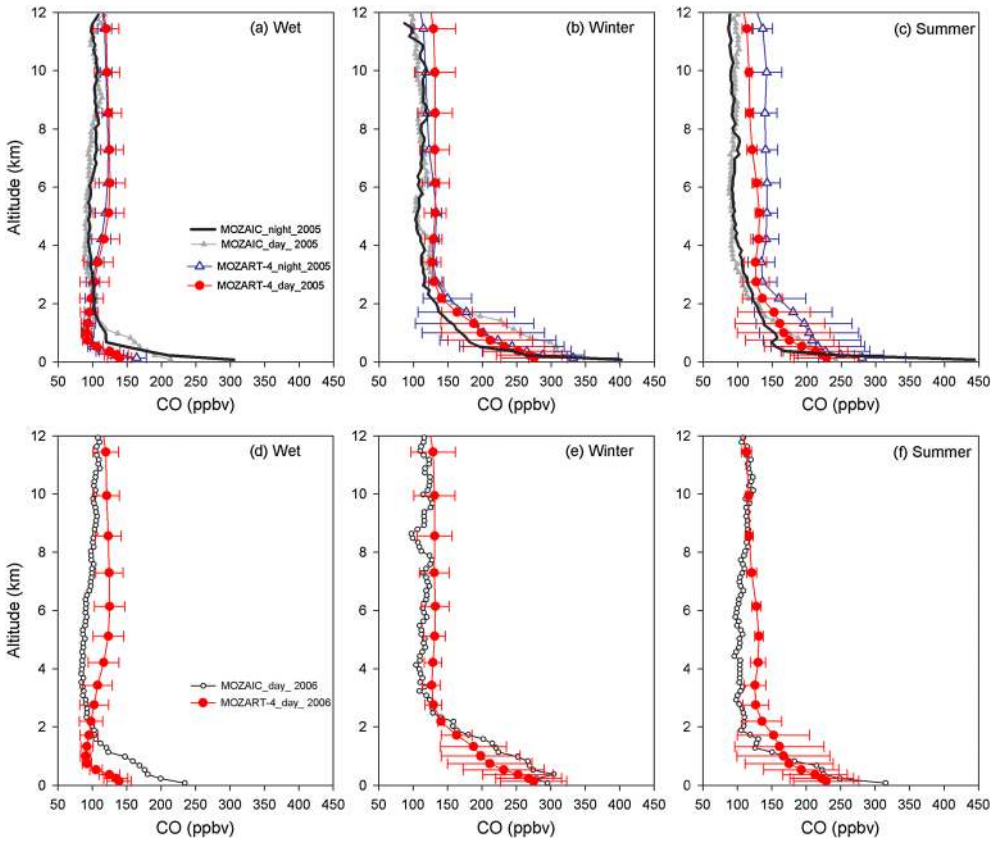

Figure 10. Comparisons between the daytime and nighttime MOZAIC and MOZART-4 profiles of CO over Bangkok during different seasons of the years (a–c) 2005 and (d–f) 2006.

5.3. Comparison of MOZAIC and MOZART-4 Profiles of O_3

[18] The average profiles of MOZAIC measurements and MOZART-4 simulations of O_3 for the three different seasons of years 2005 and 2006 are shown in Figure 7. The daytime and nighttime profiles of O_3 during year 2005 are shown separately in Figures 7a–7c. In the lower troposphere, the daytime MOZART-4 profiles of O_3 show higher values than the nighttime simulations for all the seasons of year 2005. In the lower troposphere, the MOZART-4 tends to underestimate and overestimate the daytime and nighttime observations, respectively, during year 2005. The disagreement between the observation and model is particularly significant for the nighttime profiles. Similarly, the MOZART-4 simulations do not capture the significant daytime enhancements observed in the lower tropospheric O_3 during year 2006 (see Figures 7d–7f). In the middle and upper troposphere, the MOZART-4 profiles tend to overestimate the observation during wet and winter seasons of both years. In these two seasons, the observed decline in the mixing ratio of O_3 between 9 and 12 km altitudes was not reproduced by the simulations. In the summer season, the agreement between MOZAIC and MOZART-4 gets better in the middle and upper troposphere.

[19] The box-whisker plots representing the monthly statistics of O_3 in the different regions of the troposphere (0–2, 2–4, 4–6, 6–8, 8–10, and 10–12 km) are shown in Figure 8. The mixing ratio of O_3 exhibits clear seasonal and interannual variations. The seasonal variation was strongest in the lower troposphere, but the strength of seasonality decreased at higher altitudes. Another point to be noticed in the lower troposphere is that the monthly mixing ratios of O_3 for year 2006 were higher than the values in the respective months of the year 2005. Based on the combined data for the years 2005 and 2006, the monthly mixing ratios of O_3 show minima during July–August and maxima during January–February in the lower and middle troposphere. During the year 2005, the mixing ratios of O_3 in the upper troposphere show enhancements of about 70 ppbv during April–May but the values were lowest (40–50 ppbv) during October–December. On the other hand, the enhancements in O_3 (60–70 ppbv) at 6–12 km during October–December of year 2006 were not present during the same period of year 2005. The mixing ratios of O_3 between 6 and 12 km altitudes during September–November of year 2006 were 10–15 ppbv higher than the values observed during the same period of year 2005. The box-whisker plots representing the monthly statistics of CO in the different regions of the troposphere are shown in Figure 9. We have already published the discussion of CO distributions over Bangkok [*Sahu et al.*, 2013].

[20] In Figures 8 and 9, the monthly mean MOZART-4 simulation data are also plotted for the comparison. In a first approximation, however qualitatively, the monthly simulations tend to capture the seasonality observed in the mixing ratio of O_3 in the different regions of the troposphere. In the lower troposphere, MOZART-4 agrees well during year 2005 but underestimates the observations during year 2006. This could be due to the coarse grid spacing and uncertainties in modeling the horizontal and vertical transport in the PBL region. In the

middle and upper troposphere, MOZART-4 overestimates the observations for both the years 2005–2006. In this region of the troposphere, the simulated monthly mixing ratios of O_3 during September–November of year 2006 were higher by ~10 ppbv compared to the same period of year 2005. The monthly ratios of $(O_3)_{MOZART\text{-}4}/(O_3)_{MOZAIC}$ varied in the ranges of 0.4–1.4, 0.8–1.8, 0.8–1.4, 0.8–1.2, and 0.9–2.0 at 0–2, 2–4, 4–6, 6–8, 8–10, and 10–12 km altitudes, respectively.

5.4. Comparison of MOZAIC and MOZART-4 Profiles of CO

[21] The average MOZAIC and MOZART-4 profiles of CO for the three different seasons are shown in Figure 10. The daytime and nighttime profiles of CO during year 2005 are shown separately in Figures 10a–10c. In the lower troposphere, the daytime MOZART-4 profiles of CO show lower values than the nighttime simulations for all the seasons of year 2005. Near the surface, the differences between the daytime and nighttime simulations were about 30 ppbv in the wet season and about 50 ppbv during dry months. In the PBL region, the MOZART-4 underestimates both the daytime and nighttime observations during all the seasons of year 2005. In the free troposphere, the MOZART-4 tends to overestimate both daytime and nighttime profiles. Overall, the disagreement between the observation and model is particularly significant for the nighttime profiles. Similarly, the MOZART-4 simulations of CO underestimate the observations in the lower troposphere during year 2006 (see Figures 10d–10f). On the other hand, the agreement between MOZAIC and MOZART-4 in the upper troposphere gets better during all the seasons of year 2006. However, depending on the regions of the troposphere, the monthly ratio of $CO_{MOZART\text{-}4}/CO_{MOZAIC}$ varied in the ranges of 0.6–0.9 and 0.8–1.3, respectively. The disagreement between the observation and model could partly be attributed to rather coarse resolution of MOZART simulations. The mixing ratios of O_3 and CO at Bangkok show significant diurnal variation but MOZAIC profiles were measured at specific time of day [*Zhang and Kim Oanh*, 2002; *Sahu et al.*, 2011; *Nedelec et al.*, 2003]. Therefore, lack of diurnal variability information in the observations can also be a key cause of the differences between the model and observation. The uncertainties in emissions and local dynamical processes over Bangkok can also be important factors. Other chemical transport model studies have also underestimated CO in urban PBL regions of Europe and Asia by as much as 39% due to the coarse resolution [*Chen et al.*, 2009; *Ordonez et al.*, 2010]. The uncertainties in CO can also be due to underestimated biogenic emissions in the model.

6. Discussion

6.1. Impact of Biomass Burning and Long-Range Transport

[22] The Along Track Scanning Radiometer (ATSR) fire count data have been used to investigate the spatiotemporal variation of biomass burning over different regions of the world. The method of detection and other details of the ATSR fire data can be found elsewhere [*Buongiorno et al.*, 1997; *Arino et al.*, 2001]. The seasonal fire count maps for S-SE Asia region during the years 2005 and 2006 are shown in Figure 11. In the wet season, the major biomass-burning activities were detected only in the Southern Hemisphere regions of S-SE Asia. The peat fires make the highest contribution among the other categories of biomass burning in Indonesia [*Langmann and Heil*, 2004]. In the winter season, the major fires remained very active in Indonesia but were also detected in the Northern Hemisphere regions of SE Asia (e.g., Thailand, Burma). In this season (winter), the biomass-burning activities in Thailand during the year 2006 were significantly lower than those during the year 2005. More importantly, the biomass-burning activities detected over Indonesia and Malaysia during the late wet and early winter of year 2006 were much higher than those in the same

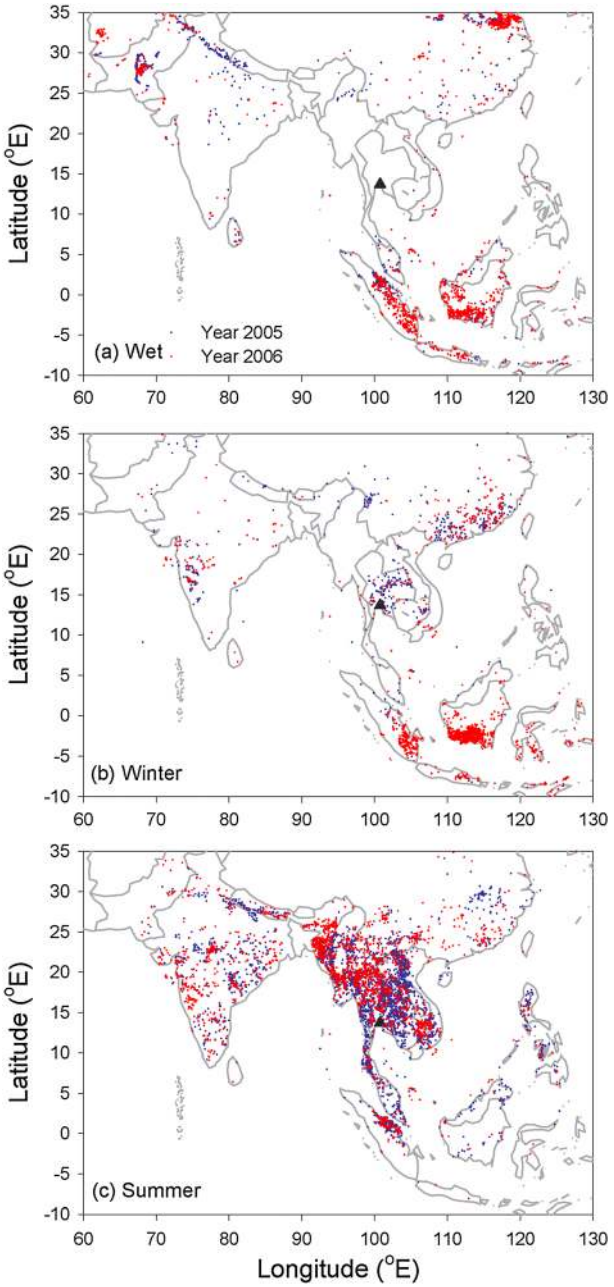

Figure 11. Maps of the ATSR fire count data detected over South and Southeast Asia (S-SE Asia) during different seasons of the years 2005 and 2006.

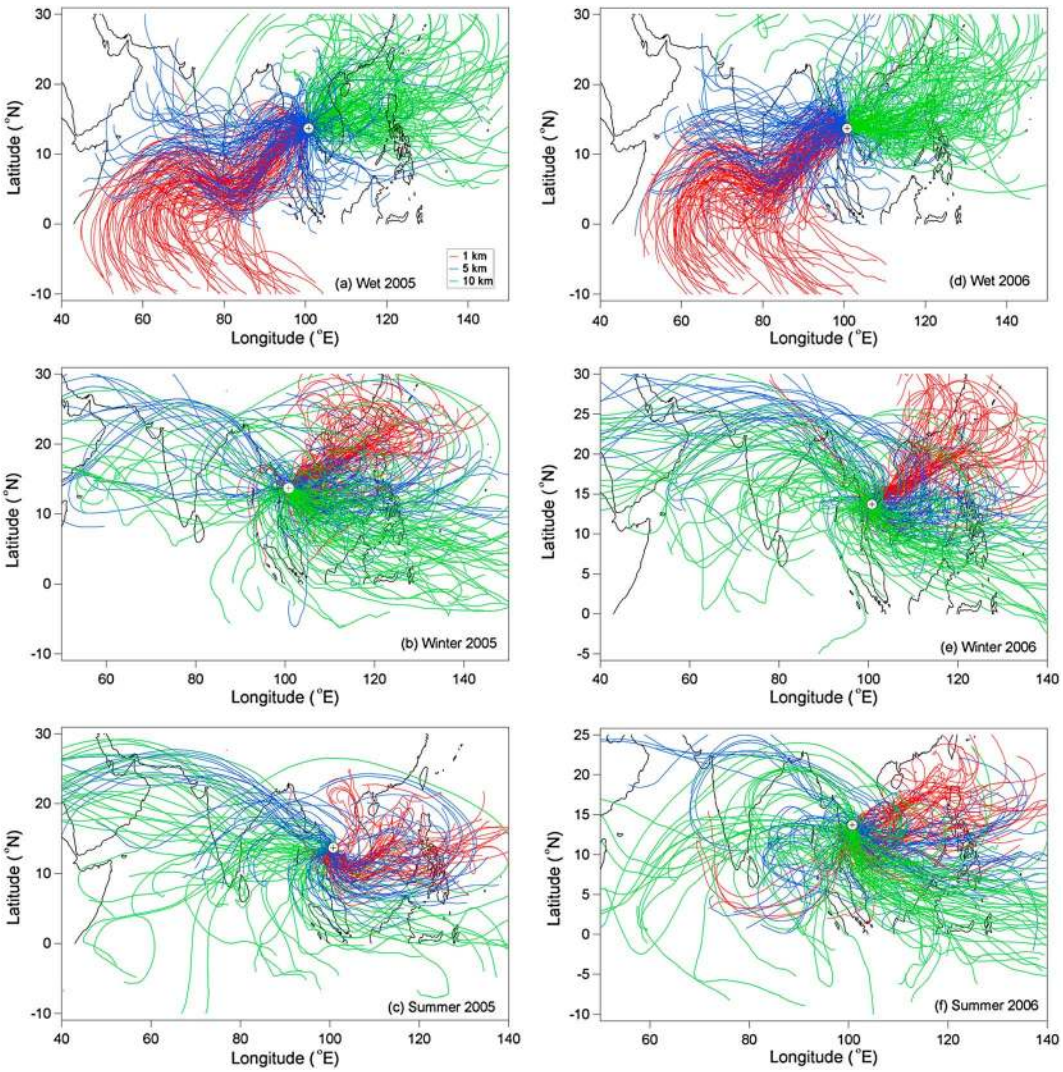

Figure 12. Back trajectory plots at 1, 5, and 10 km altitudes over Bangkok (encircled cross) during different seasons of the years 2005 and 2006.

period of year 2005. These year-to-year differences in the biomass-burning activities were caused mainly by the prevailing El Niño phenomenon during 2006. During the summer season of both years, the fire count maps show widespread biomass burning in the S-SE Asia. The number of hot spots detected in Thailand during the summer of year 2006 was lesser than those during the same season of year 2005.

[23] The monthly biomass-burning emission estimates of CO and NO_x and the fire count data over S-SE Asia during the years 2005 and 2006 were analyzed. The emission data of CO and NO_x were taken from the GFED inventory [*van der Werf et al*., 2006, 2010]. Typically, the emission and fire data show bimodal seasonality with the primary peak from February to May and the secondary peak from July to September. The primary mode is due to the biomass burning in the Northern Hemisphere parts of S-SE Asia while the secondary mode is attributed to the Southern Hemisphere parts of S-SE Asia. However, exceptionally high biomass-burning emissions of CO and NO_x during the October to November period of year 2006 were caused by the El Niño. In the month of November 2006, the emissions of CO and NO_x were highest at about 42 Tg and 0.35 Tg N, respectively. In Thailand, the highest biomass burning was detected during the February–March period. In India, the biomass burning occurs from February to May but the month of April experiences the highest activities. In summary, the fire count data detected over S-SE Asia reveal large regional, seasonal, and year-to-year variations of biomass-burning emissions. However, their roles on the vertical distributions of O_3 and CO over Bangkok depend on the pattern of long-range transport.

[24] The back trajectory models have been used to track the origin and long-range transport of air masses. The isentropic back trajectories were calculated using the Japanese 25 Year Reanalysis data (JRA-25, 6 h, $1.25° \times 1.25°$) [*Onogi et al*., 2007]. The JRA-25 covered only 26 years from 1979 to 2004. The Japan Meteorological Agency Climate Data Assimilation System (JCDAS) analysis data have been operational since 2005 and used in the present study. The JCDAS uses the common technique as JRA-25, but since it is operational day by day, only real-time observation data were assimilated. The advection algorithm used in the trajectory calculation is the same as described in *Draxler and Hess* [1997]. The trajectories were calculated for a total run time of 168 h (7 days) at 1, 5, and 10 km altitudes with a time step

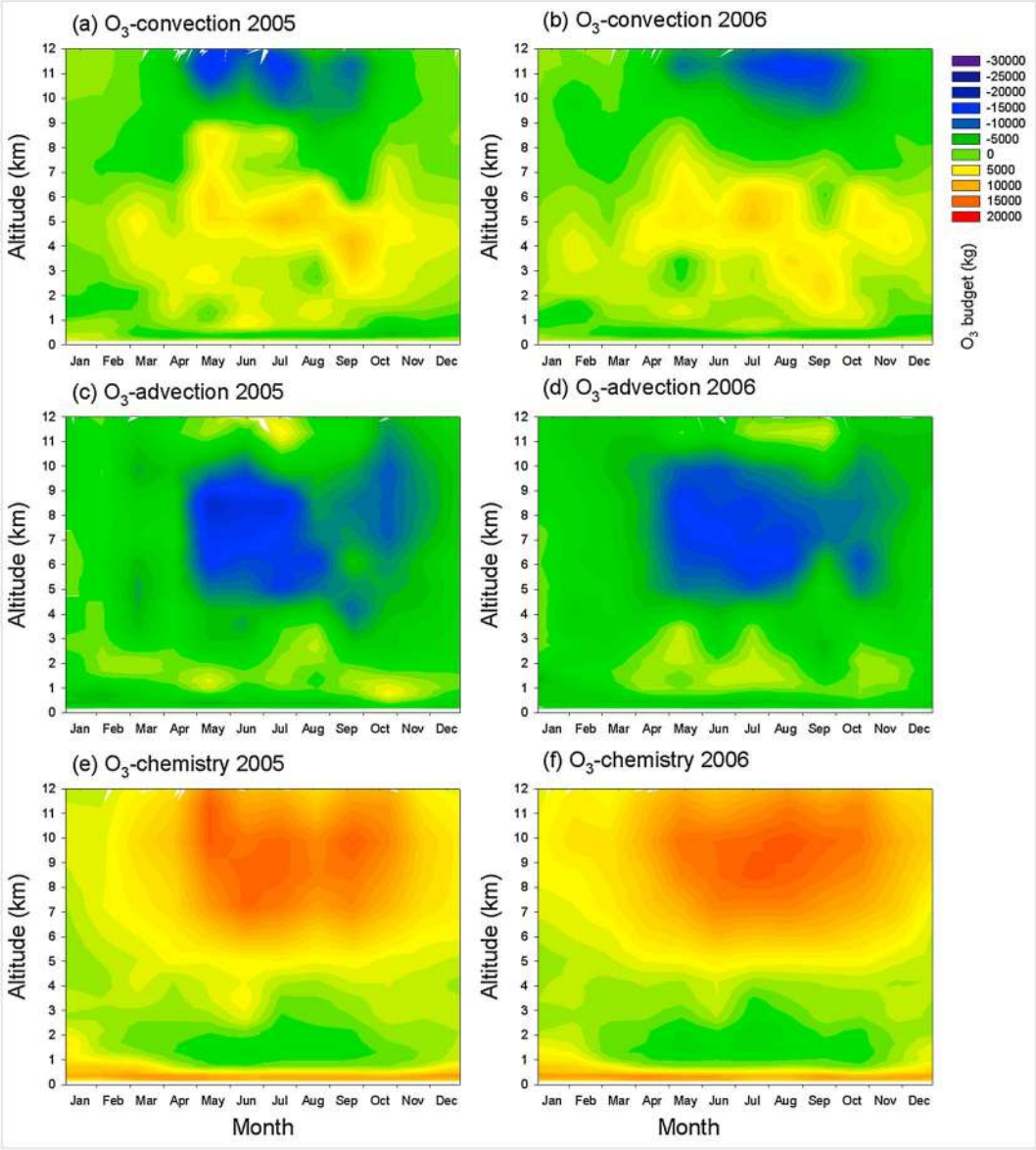

Figure 13. Seasonal contour plots of O_3 mass budget due to convection, advection, and chemistry over Bangkok during the years 2005 and 2006.

of 5 min. As shown in Figure 12, the origin and pathway of trajectories arriving over Bangkok show very clear and systematic seasonal variation during both years.

[25] In the wet season, the lower troposphere is influenced by the transport of cleaner air from the southern Indian Ocean due to the prevailing winds from the SW direction. Although not shown in the plots, the ambient pressure along the trajectories suggests that the air masses were confined within the marine boundary layer (MBL) of the Indian Ocean before they arrived over Bangkok. The flow of cleaner marine air masses in the lower troposphere could be the major cause for the low levels of O_3 and CO in the wet season. In the winter season, the back trajectories arriving in the lower troposphere show the impact of continental air from the NE direction. The trajectories at 1 km altitude were traced to have originated in the free troposphere over the eastern continental regions of China where activities of biomass burning were also significant. In the summer season, the trajectories were originated over the Pacific Ocean and arrived over Bangkok from the SE and SW directions in the lower troposphere. The local biomass-burning activities were most extensive in the summer. In spite of the flow of cleaner air from SE/SW directions, the highest mixing ratios of O_3 and CO suggest the predominance of local emissions than the transport in PBL during the summer season.

[26] The back trajectories at 5 km altitude originated over the Arabian Sea and Bay of Bengal and did not pass through major source regions in the wet season. In the winter season, the back trajectories originated over Pacific Ocean but passed over the fire active regions of Indonesia. During both winter and summer seasons, the back trajectories were mostly originated over the Pacific Ocean but some were also traced to the Indo-Gangetic Plain (IGP). The higher levels of O_3 and CO in the middle troposphere could be due to the transport of polluted air from both Indonesia and IGP. The patterns of long-range transport remained the same during

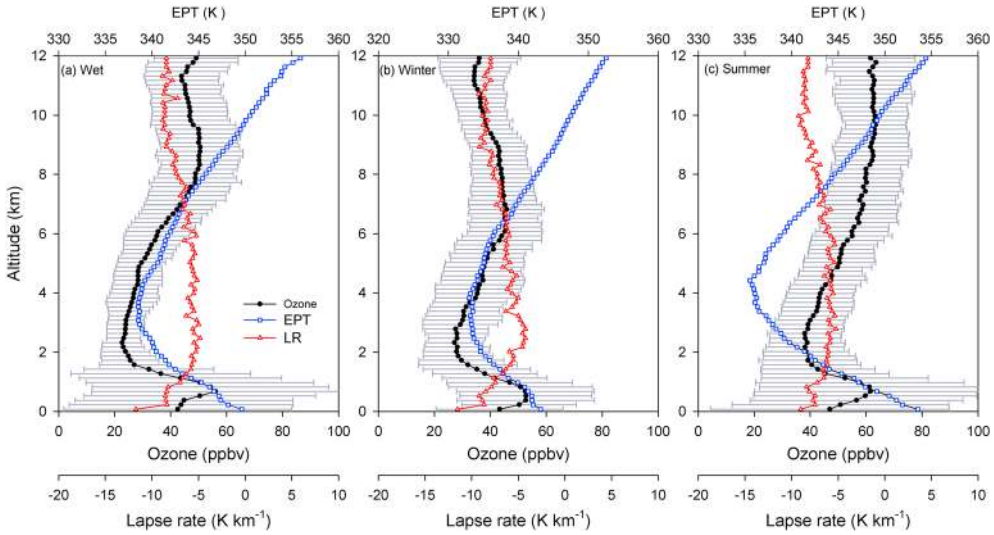

Figure 14. Seasonal mean vertical profiles of O_3, equivalent potential temperature (EPT), and lapse rate (LR) over Bangkok based on MOZAIC data during the years 2005 and 2006.

years 2005 and 2006, hence the impacts of IGP outflow for both years over Bangkok. Consequently, the enhancements in the mixing ratios of O_3 and CO particularly during the October and November months of year 2006 could be attributed to the extensive biomass burning in the Indonesian region.

[27] The mixing ratios of O_3 in the upper troposphere were about 10–20 ppbv lower than the peak values in the middle troposphere. The corresponding profiles of RH between 9 and 12 km altitudes tend to attain the values measured in PBL over Bangkok. The back trajectories arriving at 10 km altitude originated over the oceanic regions of the East China Sea, Pacific Ocean, and southern Indian Ocean during wet, winter, and summer seasons. Therefore, the absence of significant continental influence can result in declined mixing ratios of O_3 and CO between 9 and 12 km altitudes. Moreover, the lower levels of these trace gases were associated with the higher RH values (>50%) confirming the influence of cleaner ocean air masses. The interplay between convective and nonconvective transport can explain many aspects including seasonal changes in the distributions of various trace species [*Hess*, 2005]. The role of convective outflow in the distributions of O_3 and CO between 9 and 12 km altitudes has been investigated in section 6.3.

6.2. Mass Diagnostics of O_3

[28] The factors controlling the tropospheric O_3 budget have been investigated for several decades; nevertheless, there are still major uncertainties regarding several physical and chemical processes [*Lawrence et al.*, 2003]. The contributions of the different atmospheric processes controlling the vertical distribution of O_3 are diagnosed using the MOZART-4. The major processes are the three-dimensional advection derived from the large-scale meteorological fields, parameterized convection, net chemical production, and loss of O_3. Convection is parameterized using the *Hack* [1994] scheme for shallow and midlevel convection and a modified scheme by *Zhang and McFarlane* [1995] for the deep moist convection. In the present study, we have examined the role of convection, advection, and chemistry in the monthly simulations of O_3 over Bangkok (Figure 13).

[29] In the PBL region, the contributions of convection and advection were negative but positive due to chemistry during all the seasons. In the middle troposphere, the convection and chemistry show positive tendency but the contribution of advection was negative. Particularly during the summer and wet seasons, the chemical production was found to be balanced by the loss due to strong advection between 6 and 9 km altitudes. These features in the middle troposphere were particularly prominent during the late summer and wet seasons. In the upper troposphere, the convective and chemical processes show negative and positive contributions, respectively. In the middle and upper troposphere, the strong contributions of positive chemical production and loss due to convection were extended to early winter season of year 2006. Otherwise, the major features of mass diagnosis of O_3 over Bangkok remained almost similar during both years.

6.3. Impact of Convection on Distribution of O_3

[30] The field observations have shown efficient redistribution of tropospheric O_3 by the deep convection in the tropics [*Choi et al.*, 2005; *Sahu and Lal*, 2006]. There can be about 30% increase in the column tropospheric O_3 due to the convective transport of O_3 precursors, specifically NO_x to the upper troposphere [*Pickering et al.*, 1992]. On the other hand, the downdrafts of O_3-rich air from the free troposphere to the PBL and MBL regions can result in a net decrease of column O_3 [*Sahu and Lal*, 2006]. The meteorological parameters such as temperature, pressure, and water vapor are not conserved during convective updraft and downdraft. However, the value of θ_e remains conserved in adiabatic processes for both dry and moist air. The surface sensible and latent heat fluxes are the main sources of θ_e, while the radiative cooling is a primary sink in the troposphere [*Betts et al.*, 1992]. Therefore, the tropical troposphere is characterized by a decrease in θ_e and an increase in O_3 with altitude [*Folkins et al.*, 1999; *Betts et al.*, 2002]. Vertical profile of LR provides the information about the static stability of air mass. In this study, we have calculated the profiles of both θ_e and LR using MOZAIC data from the following equations:

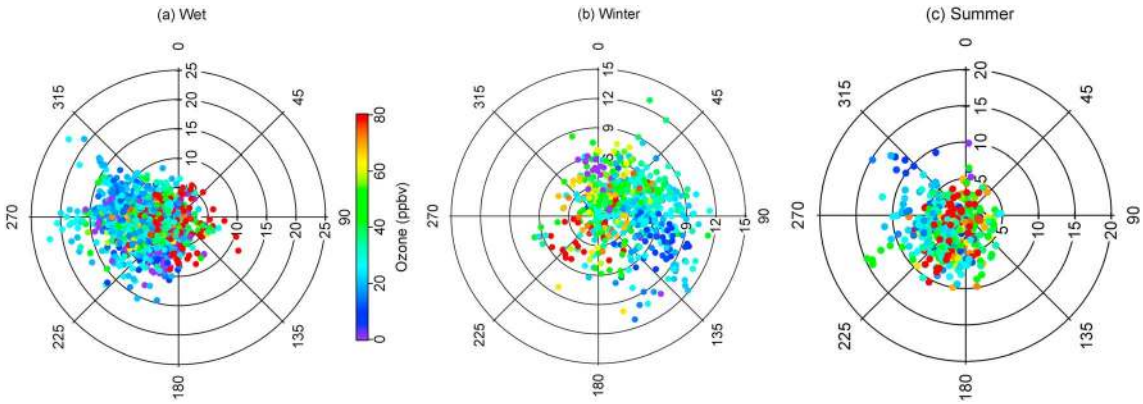

Figure 15. Polar plots of wind parameters (wind speed, m s^{-1}) and wind direction (deg) coded with the mixing ratio of O_3 in the lower troposphere (<2 km altitudes) over Bangkok during the (a) wet, (b) winter, and (c) summer seasons of the years 2005 and 2006.

$$\mathrm{EPT}\,(\theta_e) = \left(T + \frac{q \times L}{C_p}\right) \times \left(\frac{p_0}{p}\right)^{\frac{R}{C_p}} \quad (1)$$

$$\text{Lapse Rate (LR)} = \left(\frac{\mathrm{d}T}{\mathrm{d}z}\right) \quad (2)$$

[31] In equations (1) and (2), the parameters are T temperature, q specific humidity, p_0 pressure at surface, p pressure at any altitude (z), L latent heat (2.54×10^6 J kg^{-1}), R universal gas constant (287 J K^{-1}), and C_p specific heat capacity (1004 J K^{-1}). As described below, the value of θ_e increases and decreases with height in convectively stable and unstable air parcels, respectively.

$$\frac{\partial \theta_e}{\partial z} > 0 \ \text{(Stable)}$$
$$\frac{\partial \theta_e}{\partial z} = 0 \ \text{(Neutral)}$$
$$\frac{\partial \theta_e}{\partial z} < 0 \ \text{(Unstable)}$$

[32] The average vertical profiles of θ_e, LR, and O_3 over Bangkok for the wet, winter, and summer seasons are shown in Figure 14. In a tropical site such as Bangkok, the surface layer is potentially unstable due to the source of H_2O and strong solar heating. The average values of θ_e near the surface were 350 ± 4, 343 ± 8, and 354 ± 7 K which correspond to convective outflow between 9 and 12 km altitudes. In the convective system, the maximum attainable height of a convective air mass is the height at which θ_e almost becomes similar to the value at surface. Incidentally, the O_3 mixing ratios of 42–47 ppbv in the upper troposphere are similar to those observed near the surface at Bangkok during wet and winter seasons. The minimum in potential temperature (θ) lapse rate of about 5 K km^{-1} also marks the maximum impact of convection at 9–12 km altitudes over Bangkok. Therefore, the decrease in O_3 mixing between 9 and 12 km altitudes could be due to the destruction of O_3 in cloud and updraft of O_3-depleted air from the surface. In the tropics, the altitudes between 9 and 12 km are almost solely associated with deep convective clouds and their anvils [*Folkins et al.*, 1999].

[33] In the PBL region, the mixing ratios of O_3 and LR show correlation as both tend to increase with the altitude. The presence of stable layers at 2–6.5 km altitudes was marked by the lower environmental LR than moist (~6.5 K km^{-1}) and dry (~9.8 K km^{-1}) LR values. The minima in O_3 of about 23, 27, and 38 ppbv were associated with the minima in LR values of about −5, −4, and −4 K km^{-1} in the wet, winter, and summer seasons, respectively. The climatological seasonal variations of the stable and unstable layers over Bangkok agree with the present results [*Nodzu et al.*, 2006].

[34] In the upper troposphere, the environmental LR values of ~8.7–9.0 K km^{-1} are close to the dry adiabatic LR, confirming the impact of convective outflow of PBL air mass during all the seasons. In the summer season, the mixing ratio of about 65 ppbv at 11–12 km altitudes is significantly high compared to the surface value of about 47 ppbv, which indicates the additional contribution of O_3 from other processes. One of the possible reasons could be the efficient transport of precursor gases from the PBL to the upper troposphere [*Pickering et al.*, 1992; *Kita et al.*, 2002]. The convective outflow of precursors from local sources, mainly from biomass burning in summer, can enhance the photochemical formation of O_3 in the upper troposphere. This discussion agrees with the fact that the cumulonimbus clouds are preferentially distributed within a deep outflow layer (10–17 km), while the outflow from the shallow cumuli is distributed within a shallow outflow layer (2–5 km) [*Folkins and Martin*, 2005]. However, the

Table 3. Statistics (Average ± Standard Deviation) of O_3 and Meteorological Parameters in Different Wind Sectors in the Lower Troposphere (<2 km Altitudes) Over Bangkok

Wind Sector	Wind Speed (m s^{-1})	Temperature (°C)	Relative Humidity (%)	Ozone (ppbv)
N-NE	3.5 ± 1.7	22.4 ± 6	71 ± 19	53 ± 30
E-NE	4.8 ± 2.3	20.1 ± 5	78 ± 14	35 ± 19
E-SE	5.4 ± 2.8	20.1 ± 5	83 ± 12	46 ± 41
S-SE	4.5 ± 2.3	23.2 ± 4	74 ± 15	52 ± 42
S-SW	5.7 ± 2.7	22.4 ± 5	78 ± 12	43 ± 34
W-SW	7.3 ± 2.7	20.0 ± 4	82 ± 10	39 ± 26
W-NW	7.8 ± 4.3	20.1 ± 5	79 ± 12	30 ± 21
N-NW	4.2 ± 2.1	22.2 ± 5	74 ± 16	43 ± 26

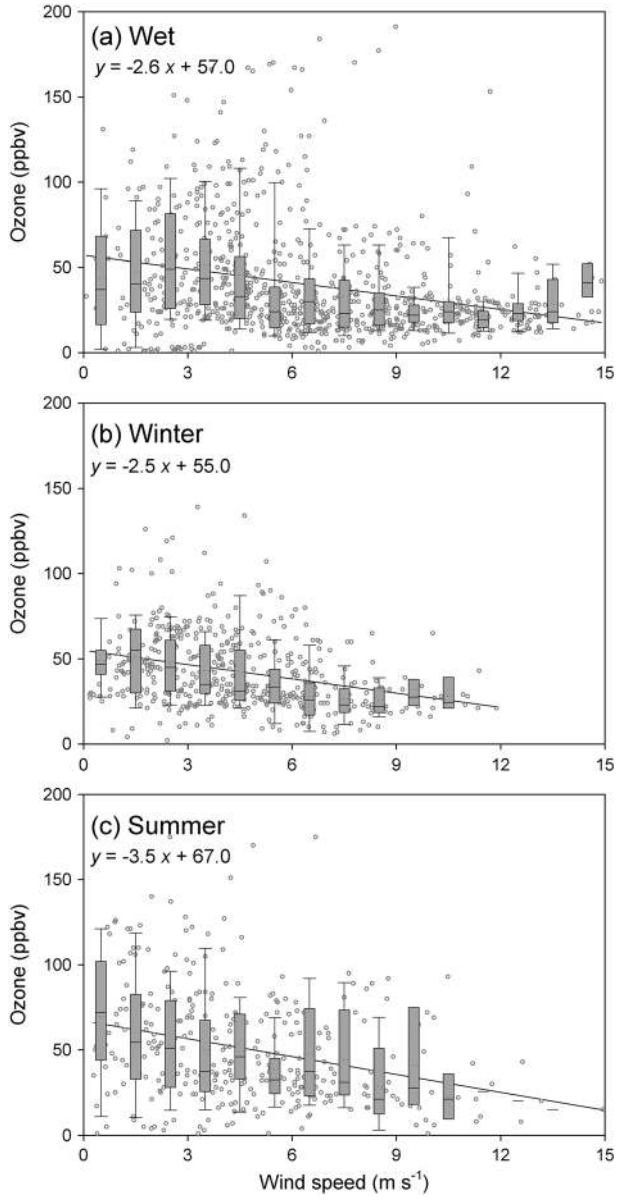

Figure 16. The scatterplots and box-whisker plots showing the dependencies of the mixing ratio of O_3 on wind speed during the wet, winter, and summer seasons.

MOZART-4 simulations do not tend to capture these features in O_3 over Bangkok caused by the convective motions.

6.4. Impact of Local Winds on O_3 in Lower Troposphere

[35] Meteorological characteristics of the PBL region are key determinants of the dispersion, transportation, and accumulation of atmospheric pollutants. Several meteorological factors can influence the distribution of O_3 in the lower troposphere. Variations in the meteorological parameters were observed to play important roles in the distributions of primary and secondary pollutants in many urban areas. For example, the direction and magnitude of the wind have been observed to affect O_3 concentrations [*Husar and Renard*, 1997]. *Sahu et al*. [2011, 2013] have shown that the surface concentrations of CO, black carbon (BC), and organic carbon (OC) aerosols in Bangkok show strong dependencies with the wind speed. However, quantitative estimation of different controlling factors requires detailed studies using regional-scale models [*Verma et al*., 2010].

[36] In this study, we have investigated the dependence of O_3 mixing ratio on the wind speed in the lower troposphere (<2 km). The polar plots of wind parameters, color coded with the mixing ratio of O_3, for the three different seasons are shown in Figure 15. As shown in Figure 15a, the mixing ratios of O_3 were mostly influenced by the winds from SW direction in the wet season. The strong winds (10–20 m s^{-1}) of cleaner marine air could have caused significant dilution of O_3 over Bangkok. However, occasionally in this season, the higher levels of O_3 were observed during the episodes of stagnant weather. In the dry season, the competing effects of sea breeze (southerly) and NE monsoon result in the low to calm wind conditions over Bangkok, hence reducing the dispersion. In the winter season, the influence of dilution was less pronounced as O_3 remained high due to flow of continental air from the NW-NE sectors (see Figure 15b). In the summer season, the winds remained calm and episodes of high O_3 were more frequent compared to the other seasons caused by widespread biomass burning in the surrounding areas of Bangkok (see Figure 15c). The higher surface temperature and accumulation of precursor gases emitted from local sources result in increased rate of photochemical production of O_3 in the summer season. The statistics of O_3 and meteorological parameters analyzed for the different wind sectors in the lower troposphere over Bangkok are presented in Table 3. During the N-NE wind flow, the mixing ratio of O_3 was highest at 53 ± 30 ppbv when wind speed was recorded to be lowest (3.5 m s^{-1}). In the W-NW sector, the mixing ratio of O_3 was lowest at 30 ± 21 ppbv, which coincided with the strong wind flow of 7.8 m s^{-1}.

[37] The dependencies of O_3 on the magnitude of wind speed for the different seasons are shown in Figure 16. In the lower wind speed regime (<5 m s^{-1}), the mixing ratio of O_3 tends to increase with the wind speed. In the higher wind flow regimes (>5 m s^{-1}), the level of O_3 decreases and also shows weaker dependence with the wind speed. The O_3-wind relation varies with the season and magnitude of the wind; overall, the mixing ratio of O_3 decreased with the increases in wind speed. The regression analysis of average O_3 versus wind speed (averaged for a bin of 1.0 m s^{-1}) data shows very good linear fits during the wet, winter, and summer seasons, respectively. The slopes of $\Delta O_3/\Delta$(wind speed) were −2.6, −2.5, and −3.5 ppbv/m s^{-1} during the wet, winter, and summer seasons, respectively. The decline of O_3 with the wind speed can be interpreted as evidence of local source contributions, since higher wind speeds cause increasing dilution of local production of O_3. On the other hand, if the mixing ratio is found to be constant with wind speed, then the local contribution is not substantial. The actual origin of the regional O_3 is identified only vaguely through the directional analysis of wind parameters. The mixing ratio of O_3 does not exhibit significant relation with the wind speed in the middle and upper troposphere over Bangkok.

7. Summary and Conclusions

[38] The characteristics of tropospheric O_3 over Bangkok have been presented based on the MOZAIC measurements

and simulations using MOZART-4 for the years 2005 and 2006. We have investigated the seasonal and year-to-year variations of O_3 using CO, back trajectory, fire count, and meteorological data. The three different seasons of wet, winter, and summer characterized by distinct variations in the meteorological parameters are linked to the movement of the ITCZ. The observations in the wet season were influenced by the flow of cleaner marine air due to prevailing SW winds, while the winds from NE and NW directions transported the continental pollutants during the winter season. The local air masses that originated mainly over the continental and marine regions of SE Asia prevailed in the summer season. In the middle troposphere, the air masses passed over the fire-affected areas of Indonesia during the late wet and early winter months. In the wet season, the major activities of biomass burning were located in the Southern Hemisphere regions of S-SE Asia. In the winter season, the major activities of biomass burning were located in the Northern Hemisphere regions of SE Asia. The activities of biomass burning during summer were extensive and widespread in the S-SE Asia. Indonesia experienced extensive biomass burning from September to November of the year 2006 due to El Niño, while 2005 was a normal year. The emissions of O_3 precursors like CO and NO_x from biomass-burning sources in S-SE Asia during September to November of the year 2006 were several times higher than those estimated for the same period of the year 2005.

[39] The mixing ratio of O_3 exhibits strong seasonal variation with the lowest and highest values during the wet and summer seasons, respectively. In the PBL region, the nighttime and daytime mixing ratios of O_3 were 20–40 and 40–80 ppbv, respectively, during the year 2005. The differences were also observed in the mixing ratios of CO, however, with the high and low values during the day and night, respectively. In the free troposphere, the differences between the daytime and nighttime profiles of O_3 and CO were not significant. The mixing ratios of O_3 were lowest between 2 and 4 km altitudes with the averages of 25, 30, and 40 ppbv for the wet, winter, and summer seasons, respectively. The back trajectory and fire count data indicate the role of extensive biomass burning in Indonesia during the year 2006 contributing to large year-to-year variations in the profiles of O_3 and CO over Bangkok.

[40] In the wet and winter seasons, the mixing ratios of O_3 decreased with the altitude in the upper troposphere. The vertical profiles of equivalent potential temperature and lapse rate indicate the roles of convection and static stability in the distributions of O_3 over Bangkok. The declines of O_3 in the lower and upper troposphere were associated with the shallow and deep convections, respectively. The environmental LR values of ~8.7–9.0 K km^{-1} are close to the dry adiabatic LR confirming the impact of convective outflow of PBL air mass between 9 and 12 km altitudes. The MOZART-4 simulations underestimated the observations of O_3 and CO in the PBL region, but the agreement becomes better in the free troposphere. The MOZART-4 simulations captured the differences between the daytime and nighttime profiles of O_3 and CO but failed to reproduce their decline in the upper troposphere. The monthly ratios of $(O_3)_{MOZART\text{-}4}/(O_3)_{MOZAIC}$ varied in the ranges of 0.4–2.0 depending on the region of the troposphere. The mass diagnostics of O_3 indicate the negative contributions of convection and advection but positive due to chemistry in the PBL region. In the middle troposphere, the extended contribution of positive chemical production during the early winter months of the year 2006 was due to the El Niño. The mixing ratio of O_3 in the PBL region depends on local wind but no clear dependencies were observed in the free troposphere. Overall, the mixing ratio of O_3 decreased with the increase in the magnitude of wind speed. The relationship between O_3 and wind speed varies with the season with the $\Delta O_3/\Delta$(wind speed) slopes of −2.6, −2.5, and −3.5 ppbv/m s^{-1} during the wet, winter, and summer seasons, respectively. The declining mixing ratio of O_3 with wind speed indicates the contributions from local photochemical production.

[41] **Acknowledgments.** The authors acknowledge for their strong support the European Commission, Airbus, CNRS-France, FZJ-Germany, and the airlines (Lufthansa, Air France, Austrian, and the former Sabena who carry free of charge the MOZAIC instrumentation since 1994). The ATSR World Fire Atlas data have been taken from Ionia products of the European Space Agency.

References

Allan, R., J. Lindesay, and D. E. Parker (1996), *El Niño Southern Oscillation and Climatic Variability*, pp. 416, CSIRO, Collingwood, Victoria, Australia.

Arino, O., M. Simon, I. Piccolini, and J. M. Rosaz (2001), *The ERS-2 ATSR-2 World Fire Atlas and the ERS-2 ATSR-2 World Burnt Surface Atlas Projects, Paper Presented at 8th ISPRS Conference on Physical Measurement and Signatures in Remote Sensing*, European Space Agency, Aussois, France.

Asnani, G. C. (2005), Climatology of the tropics, in *Tropical Meteorology*, G. C. Asnani, Pune, India, vol. 1, pp. 100–204 .

Bangkok Metropolitan Administration (2009), Green Leaf Foundation and United Nations Environment Programme, *Bangkok Assessment Report on Climate Change 2009*. BMA, GLF and UNEP, Bangkok.

Betts, A. K., R. L. Desjardins, and J. I. MacPherson (1992), Budget analysis of the boundary layer grid flights during FIFE 1987, *J. Geophys. Res.*, *97*, 18,533–18,546.

Betts, A. K., L. V. Gatti, A. M. Cordova, M. A. F. Silva Dias, and J. Fuentes (2002), Transport of ozone to the surface by convective downdrafts at night, *J. Geophys. Res.*, *107*(D20), 8046, doi:10.1029/2000JD000158.

Buongiorno, A., O. Arino, C. Zehner, P. Colagrande, and P. Goryl (1997), ERS-2 monitors exceptional fire event, *Earth Obs. Q.*, *56*, 1–6.

Chan, C. Y., L. Y. Chan, W. L. Chang, Y. G. Zheng, H. Cui, X. D. Zheng, Y. Qin, and Y. S. Li (2003), Characteristics of a tropospheric ozone profile and implications for the origin of ozone over subtropical China in the spring of 2001, *J. Geophys. Res.*, *108*(D20), 8800, doi:10.1029/2003JD003427.

Chandra, S., J. R. Ziemke, and R. V. Martin (2003), Tropospheric ozone at tropical and middle latitudes derived from TOMS/MLS residual: Comparison with a global model, *J. Geophys. Res.*, *108*(D9), 4291, doi:10.1029/2002JD002912.

Chen, D., Y. Wang, M. B. McElroy, K. He, R. M. Yantosca, and P. Le Sager (2009), Regional CO pollution and export in China simulated by the high-resolution nested-grid GEOS-Chem model, *Atmos. Chem. Phys.*, *9*, 3825–3839.

Choi, Y., Y. Wang, T. Zeng, R. V. Martin, T. P. Kurosu, and K. Chance (2005), Evidence of lightning NO_x and convective transport of pollutants in satellite observations over North America, *Geophys. Res. Lett.*, *32*, L02805, doi:10.1029/2004GL021436.

Chuersuwan, N., S. Nimrat, S. Lekphet, and T. Kerdkumrai (2008), Levels and major sources of PM2.5 and PM10 in Bangkok Metropolitan Region, *Environ. Int.*, *34*, 671–677, doi:10.1016/j.envint.2007.12.018.

Cooper, O. R., et al. (2004), A case study of transpacific warm conveyor belt transport: Influence of merging airstreams on trace gas import to North America, *J. Geophys. Res.*, *109*, D23S08, doi:10.1029/2003JD003624.

Cooper, O. R., et al. (2010), Increasing springtime ozone mixing ratios in the free troposphere over western North America, *Nature*, *463*, 344–348, doi:10.1038/nature08708.

Department of Land Transport (DLT) (2008), Transport statistics, Bangkok, (Available at http://apps.dlt.go.th/statistics_web/statistics.html.).

Department of Land Transport (DLT) (2010), Statistic: Number of vehicle registered in Bangkok as of 31 December 2010, Bangkok, (Available at http://apps.dlt.go.th/statistics_web/vehicle.html.).

Draxler, R. R., and G. D. Hess (1997), Description of the HYSPLIT_4 modeling system, NOAA Tech. Memo. ERL ARL-224, 24 pp.

Emmons, L. K., et al. (2010), Description and evaluation of the Model for Ozone and Related Chemical Tracers, version 4 (MOZART-4), *Geosci. Model Dev.*, *3*(1), 43–67.

Fishman, J., K. Fakhruzzaman, B. Cros, and D. Nganga (1991), Identification of widespread pollution in the Southern Hemisphere deduced from satellite analyses, *Science*, *252*, 1693–1696.

Folkins, I., and R. V. Martin (2005), The vertical structure of tropical convection and its impact on the budgets of water vapor and ozone, *J. Atmos. Sci.*, *62*, 1560–1573.

Folkins, I., M. Loewenstein, J. Podolske, S. J. Oltmans, and M. Proffitt (1999), A barrier to vertical mixing at 14 km in the tropics: Evidence from ozonesondes and aircraft measurements, *J. Geophys. Res.*, *104*, 22,095–22,102.

Folkins, I., C. Braun, A. M. Thompson, and J. C. Witte (2002), Tropical ozone as an indicator of deep convective outflow, *J. Geophys. Res.*, *107*(D13), 4184, doi:10.1029/2001JD001178.

Forster, P. M., and K. P. Shine (1997), Radiative forcing and temperature trends from stratospheric ozone changes, *J. Geophys. Res.*, *102*, 10,841–10,856.

Fujiwara, M., K. Kita, S. Kawakami, T. Ogawa, N. Komala, S. Saraspriya, and A. Suripto (1999), Tropospheric ozone enhancements during the Indonesian Forest Fire Events in 1994 and in 1997 as revealed by ground-based observations, *Geophys. Res. Lett.*, *26*, 2,417–2,420, doi:10.1029/1999GL900117.

Fujiwara, M. K., K. Kita, T. Ogawa, S. Kawakami, T. Sano, N. Komala, S. Saraspriya, and A. Suriputo (2000), Seasonal variation of tropospheric ozone in Indonesia revealed by 5-year ground-based observations, *J. Geophys. Res.*, *105*, 1879–1888.

Gauss, M., et al. (2003), Radiative forcing in the 21st century due to ozone changes in the troposphere and the lower stratosphere, *J. Geophys. Res.*, *108*(D9), 4292, doi:10.1029/2002JD002624.

Granier, C., et al. (2004), Present and future surface emissions of atmospheric compounds, European Commission report EVK 2199900011.

Hack, J. J. (1994), Parameterization of moist convection in the NCAR Community Climate Model, CCM2, *J. Geophys. Res.*, *99*, 5551–5568, doi:10.1029/93JD03478.

Heald, C. L., D. J. Jacob, P. Palmer, M. J. Evans, G. W. Sachse, H. B. Singh, and D. R. Blake (2003), Biomass burning emission inventory with daily resolution: Application to aircraft observations of Asian outflow, *J. Geophys. Res.*, *108*(D21), 8811, doi:10.1029/2002JD003082.

Hess, P. G. (2005), A comparison of two paradigms: The relative global roles of moist convective versus nonconvective transport, *J. Geophys. Res.*, *110*, D20302, doi:10.1029/2004JD005456.

Horowitz, L. W., et al. (2003), A global simulation of tropospheric ozone and related tracers: Description and evaluation of MOZART, version 2, *J. Geophys. Res.*, *108*(D24), 4784, doi:10.1029/2002JD002853.

Husar, R. B., and W. P. Renard (1997), Ozone as a function of local wind speed and direction: Evidence of local and regional transport, Paper presented at the Air and Waste Management Association's 90th Annual Meeting and Exhibition, Toronto, Ontario, 8–13 June 1997.

Intergovernmental Panel on Climate Change (2007), *Climate Change 2007: The Physical Science Basis. Contribution of Working Group I to the Fourth Assessment Report of the Intergovernmental Panel on Climate Change*, edited by S. Solomon et al., 996 pp., Cambridge Univ. Press, Cambridge, U.K.

Kita, K., et al. (2002), Photochemical production of ozone in the upper troposphere in association with cumulus convection over Indonesia, *J. Geophys. Res.*, *107*(D3), 8400, doi:10.1029/2001JD000844, [printed 108(D3), 2003].

Kumar, R., M. Naja, G. G. Pfister, M. C. Barth, C. Wiedinmyer, and G. P. Brasseur (2012), Simulations over South Asia using the weather research and forecasting model with chemistry (WRF-Chem): Chemistry evaluation and initial results, *Geosci. Model Dev.*, *5*, 619–648.

Lal, S., L. K. Sahu, and S. Venkataramani (2007), Impact of transport from the surrounding continental regions on the distributions of ozone and related trace gases over the Bay of Bengal during February 2003, *J. Geophys. Res.*, *112*, D14302, doi:10.1029/2006JD008023.

Lamarque, J. F., et al. (2010), Historical (1850–2000) gridded anthropogenic and biomass burning emissions of reactive gases and aerosols: Methodology and application, *Atmos. Chem. Phys.*, *10*(15), 7017–7039.

Langmann, B., and A. Heil (2004), Release and dispersion of vegetation and peat fire emissions, *Atmos. Chem. Phys.*, *4*, 2145–2160.

Lawrence, M. G., R. von Kuhlmann, M. Salzmann, and P. J. Rasch (2003), The balance of effects of deep convective mixing on tropospheric ozone, *Geophys. Res. Lett.*, *30*(18), 1940, doi:10.1029/2003GL017644.

Lelieveld, J., et al. (2001), The Indian Ocean experiment: Widespread air pollution from South and Southeast Asia, *Science*, *291*(5506), 1031–1036.

Lin, M., et al. (2012), Transport of Asian ozone pollution into surface air over the western United States in spring, *J. Geophys. Res.*, *117*, D00V07, doi:10.1029/2011JD016961.

Logan, J. (1999), An analysis of ozonesonde data for the troposphere: Recommendations for testing 3-D models and development of a gridded climatology for tropospheric ozone, *J. Geophys. Res.*, *104*, 16,115–16,149, doi:10.1029/1998JD100096.

Marenco, A., et al. (1998), Measurement of ozone and water vapor by Airbus in-service aircraft: The MOZAIC airborne program, an overview, *J. Geophys. Res.*, *103*, 25,631–25,642, doi:10.1029/98JD00977.

Nara, H., H. Tanimoto, Y. Nojiri, H. Mukai, J. Zeng, Y. Tohjima, and T. Machida (2011), CO emissions from biomass burning in Southeast Asia in the 2006 El Niño year: Shipboard and AIRS satellite observations, *Environ. Chem.*, *8*, 213–223, doi:10.1071/EN10113.

Nassar, R., J. A. Logan, I. A. Megretskaia, L. T. Murray, L. Zhang, and D. B. A. Jones (2009), Analysis of tropical tropospheric ozone, carbon monoxide, and water vapor during the 2006 El Niño using TES observations and the GEOS-Chem model, *J. Geophys. Res.*, *114*, D17304, doi:10.1029/2009JD011760.

Nedelec, P., J.-P. Cammas, V. Thouret, G. Athier, J.-M. Cousin, C. Legrand, C. Abonnel, F. Lecoeur, G. Cayez, and C. Marizy (2003), An improved infrared carbon monoxide analyser for routine measurements aboard commercial Airbus aircraft: Technical validation and first scientific results of the MOZAIC III programme, *Atmos. Chem. Phys.*, *3*(5), 1551–1564.

Nodzu, M. I., S.-Y. Ogino, Y. Tachibana, and M. D. Yamanaka (2006), Climatological description of seasonal variations in lower-tropospheric temperature inversion layers over the Indochina Peninsula, *J. Clim.*, *19*(13), 3307–3319.

Ohara, T., H. Akimoto, J. Kurokawa, N. Horii, K. Yamaji, X. Yan, and T. Hayasaka (2007), An Asian emission inventory of anthropogenic emission sources for the period 1980–2020, *Atmos. Chem. Phys. Discuss.*, *7*, 6843–6902, doi:10.5194/acpd-7-6843-2007.

Olivier, J. G. J., J. A. H. W. Peters, J. Bakker, J. J. M. Berdowski, A. J. H. Visschedijk, and J. P. J. Bloos (2002), Applications of EDGAR: Emission database for global atmospheric research, *Rep.* 410.200.051. RIVM, Rijksinst. voor Volkzgezondh. en Milieu, Bilthoven, Netherlands.

Olivier, J., J. Peters, C. Granier, G. Petron, J. Müller, and S. Wallens (2003), Present and future surface emissions of atmospheric compounds, POET Rep. 2, EU Proj. EVK2-1999-00011, ACCENT, Paris. [Available at http://www.aero.jussieu.fr/projet/ACCENT/POET.php.]

Olivier, J. G. J., et al. (2005), Recent trends in global greenhouse gas emissions: Regional trends 1970–2000 and spatial distribution of key sources in 2000, *Env. Sc.*, *2*(2–3), 81–99.

Oltmans, S. J., A. S. Lefohn, J. M. Harris, I. Galbally, H. E. Scheel, G. Bodeker, E. Brunke, H. Claude, D. Tarasick, and B. J. Johnson (2006), Long-term changes in tropospheric ozone, *Atmos. Environ.*, *40*, 3156–3173, doi:10.1016/j.atmosenv.2006.01.029.

Onogi, K., et al. (2007), The JRA-25 reanalysis, *J. Meteorol. Soc. Jpn.*, *85*, 369–432, doi:10.2151/jmsj.85.369.

Ordonez, C., et al. (2010), Global model simulations of air pollution during the 2003 European heat wave, *Atmos. Chem. Phys.*, *10*(2), 789–815.

Pickering, K. E., A. M. Thompson, J. R. Scala, W. Tao, R. R. Dickerson, and J. Simpson (1992), Free tropospheric ozone production following entrainment of urban plumes into deep convection, *J. Geophys. Res.*, *97*, 17,985–18,000.

Pochanart, P., H. Akimoto, Y. Kajii, and P. Sukasem (2003), Carbon monoxide, regional-scale transport, and biomass burning in tropical continental Southeast Asia: Observations in rural Thailand, *J. Geophys. Res.*, *108*(D17), 4552, doi:10.1029/2002JD003360.

Sahu, L. K. (2012), Volatile organic compounds and their measurements in the troposphere, *Curr. Sci.*, *102*(10), 1,645–1,649.

Sahu, L. K., and S. Lal (2006), Changes in surface ozone levels due to convective downdrafts over the Bay of Bengal, *Geophys. Res. Lett.*, *33*, L10807, doi:10.1029/2006GL025994.

Sahu, L. K., S. Lal, and S. Venkataramani (2006), Distributions of O3, CO and hydrocarbons over the Bay of Bengal: A study to assess the role of transport from southern India and marine regions during September–October 2002, *Atmos. Environ.*, *40*, 4633–4645.

Sahu, L. K., S. Lal, V. Thouret, and H. G. Smit (2009a), Seasonality of tropospheric ozone and water vapor over Delhi, India: A study based on MOZAIC measurement data, *J. Atmos. Chem.*, *62*, 151–174, doi:10.1007/s10874-010-9146-1.

Sahu, L. K., Y. Kondo, Y. Miyazaki, M. Kuwata, M. Koike, N. Takegawa, H. Tanimoto, H. Matsueda, S. C. Yoon, and Y. J. Kim (2009b), Anthropogenic aerosols observed in Asian continental outflow at Jeju Island, Korea, in spring 2005, *J. Geophys. Res.*, *114*, D03301, doi:10.1029/2008JD010306.

Sahu, L. K., S. Lal, V. Thouret, and H. G. Smit (2010), Climatology of tropospheric ozone and water vapour over Chennai: A study based on MOZAIC measurements over India, *Int. J. Climatol.*, *31*, 920–936, doi:10.1002/joc.2128.

Sahu, L. K., Y. Kondo, Y. Miyazaki, P. Pongkiatkul, and N. T. Kim Oanh (2011), Seasonal and diurnal variations of black carbon and organic carbon aerosols in Bangkok, *J. Geophys. Res.*, *116*, D15302, doi:10.1029/2010JD015563.

Sahu, L. K., V. Sheel, M. Kajino, and P. Nedelec (2013), Variability in tropospheric carbon monoxide over an urban site in Southeast Asia, *Atmos. Environ.*, *68*, 243–255.

Sheel, V., S. Lal, A. Richter, and J. P. Burrows (2010), Comparison of satellite observed tropospheric NO_2 over India with model simulations, *Atmos. Environ.*, *44*(27), 3314–3321.

Sherwood, S. C., and A. E. Dessler (2003), Convective mixing near the tropical tropopause: Insights from seasonal variations, *J. Atmos. Sci.*, *60*, 2674–2685.

Srivastava, S., and V. Sheel (2012), Study of tropospheric CO and O3 enhancement episode over Indonesia during Autumn 2006 using the Model for Ozone and Related Chemical Tracers (MOZART-4), *Atmos. Environ.*, *67*(0), 53–62.

Streets, D. G., et al. (2003a), An inventory of gaseous and primary aerosol emissions in Asia in the year 2000, *J. Geophys. Res.*, *108*(D21), 8809, doi:10.1029/2002JD003093.

Streets, D. G., K. F. Yarber, J.-H. Woo, and G. R. Carmichael (2003b), Biomass burning in Asia: Annual and seasonal estimates and atmospheric emissions, *Global Biogeochem. Cycles*, *17*(4), 1099, doi:10.1029/2003GB002040.

Thompson, A. M., J. C. Witte, R. D. Hudson, H. Guo, J. R. Herman, and M. Fujiwara (2001), Tropical tropospheric ozone and biomass burning, *Science*, *291*, 2128–2132.

Thompson, A. M., et al. (2003), Southern Hemisphere Additional Ozonesondes (SHADOZ) 1998–2000 tropical ozone climatology: 1. Comparison with Total Ozone Mapping Spectrometer (TOMS) and ground-based measurements, *J. Geophys. Res.*, *108*(D2), 8238, doi:10.1029/2001JD000967.

Thouret, V., A. Marenco, P. Nédélec, and C. Grouhel (1998a), Ozone climatologies at 9–12 km altitude as seen by the MOZAIC airborne program between September 1994 and August 1996, *J. Geophys. Res.*, *103*, 25,653–25,680.

Thouret, V., A. Marenco, J. A. Logan, P. Nédélec, and C. Grouhel (1998b), Comparisons of ozone measurements from the MOZAIC airborne program and the ozone sounding network at eight locations, *J. Geophys. Res.*, *103*, 25,695–25,720.

Tipayarom, D., and N. T. Kim Oanh (2007), Effects from open rice straw burning emission on air quality in the Bangkok Metropolitan Region, *Sci. Asia*, *33*, 339–345, doi:10.2306/scienceasia1513-1874.2007.33.339.

van der Werf, G., J. T. Randerson, L. Giglio, G. J. Collatz, P. S. Kasibhatla, and A. F. Arellano (2006), Interannual variability of global biomass burning emissions from 1997 to 2004, *Atmos. Chem. Phys.*, *6*, 3423–3441, doi:10.5194/acp-6-3423-2006.

van der Werf, G. R., J. T. Randerson, L. Giglio, G. J. Collatz, M. Mu, P. S. Kasibhatla, D. C. Morton, R. S. DeFries, Y. Jin, and T. T. van Leeuwen (2010), Global fire emissions and the contribution of deforestation, savanna, forest, agricultural, and peat fires (1997–2009), *Atmos. Chem. Phys.*, *10*, 11,707–11,735, doi:10.5194/acp-10-11707-2010.

Verma, R. L., et al. (2010), Temporal variations of black carbon in Guangzhou, China, in summer 2006, *Atmos. Chem. Phys.*, *10*, 6471–6485, doi:10.5194/acp-10-6471-2010.

Vingarzan, R. (2004), A review of surface ozone background levels and trends, *Atmos. Environ.*, *38*, 3,431–3,442, doi:10.1016/j.atmosenv.2004.03.030.

Yonemura, S., H. Tsuruta, S. Kawashima, S. Sudo, L. C. Peng, L. S. Fook, Z. Johar, and M. Hayashi (2002), Tropospheric ozone climatology over Peninsular Malaysia from 1992 to 1999, *J. Geophys. Res.*, *107*(D15), 4229, doi:10.1029/2001JD000993.

Yurganov, L. N., W. W. McMillan, A. V. Dzhola, E. I. Grechko, N. B. Jones, and G. R. van der Werf (2008), Global AIRS and MOPITT CO measurements: Validation, comparison, and links to biomass burning variations and carbon cycle, *J. Geophys. Res.*, *113*, D09301, doi:10.1029/2007JD009229.

Zhang, B. N., and N. T. Kim Oanh (2002), Photochemical smog pollution in the Bangkok Metropolitan Region of Thailand in relation to O3 precursor concentrations and meteorological conditions, *Atmos. Environ.*, *36*(26), 4211–4222.

Zhang, G. J., and N. A. McFarlane (1995), Sensitivity of climate simulations to the parameterization of cumulus convection in the Canadian Climate Centre General Circulation Model, *Atmos. Ocean*, *33*, 407–446.

Zhang, L., et al. (2008), Transpacific transport of ozone pollution and the effect of recent Asian emission increases on air quality in North America: An integrated analysis using satellite, aircraft, ozonesonde, and surface observations, *Atmos. Chem. Phys.*, *8*, 6117–6136.

Zhang, L., Q. B. Li, J. Jin, H. Liu, N. Livesey, J. H. Jiang, Y. Mao, D. Chen, M. Luo, and Y. Chen (2011), Impacts of 2006 Indonesian fires and dynamics on tropical upper tropospheric carbon monoxide and ozone, *Atmos. Chem. Phys.*, *11*(21), 10,929–10,946.